NAVAL POSTGRADUATE SCHOOL
Monterey, California

AD-A274 914

THESIS

METHODS FOR IMPROVING LOW-ANGLE, LOW-ALTITUDE RADAR TRACKING ACCURACY

by

Ali Ozkara

September, 1993

Thesis Advisor :   Professor David C. Jenn

Approved for public release; distribution is unlimited.

94-02155

94 1 25 053

REPORT DOCUMENTATION PAGE

1a Report Security Classification: Unclassified	1b Restrictive Markings
2a Security Classification Authority	3 Distribution/Availability of Report
2b Declassification/Downgrading Schedule	Approved for public release; distribution is unlimited.
4 Performing Organization Report Number(s)	5 Monitoring Organization Report Number(s)

6a Name of Performing Organization Naval Postgraduate School	6b Office Symbol 3A	7a Name of Monitoring Organization Naval Postgraduate School
6c Address Monterey, CA 93943-5000		7b Address Monterey, CA 93943-5000
8a Name of Funding/Sponsoring Organization	6b Office Symbol	9 Procurement Instrument Identification Number

Address	10 Source of Funding Numbers			
	Program Element No	Project No	Task No	Work Unit Accession No

11 Title METHODS FOR IMPROVING LOW-ANGLE, LOW-ALTITUDE RADAR TRACKING ACCURACY.

12 Personal Author(s) Ali Ozkara

13a Type of Report Master's Thesis	13b Time Covered From To	14 Date of Report 1993 September 23	15 Page Count 70

16 Supplementary Notation The views expressed in this thesis are those of the author and do not reflect the official policy or position of the Department of Defense or the U.S. Government.

17 Cosati Codes			18 Subject Terms (continue on reverse if necessary and identify by block number)
Field	Group	Subgroup	serial search acquisition, spread-spectrum, communications

19 Abstract

    This thesis studies the problem of low-angle, low-altitude target tracking where the presence of multipath causes large angle errors. The problem is examined for a low sidelobe monopulse radar over a flat earth. A detailed multipath model is used to simulate the reflecting surface and the reflected signal is included in the monopulse processing simulation. Using this model the tracking error is obtained, and two multipath error reduction techniques are evaluated. The first method uses frequency agility to measure the angle over a wide frequency range. By averaging the results of many frequencies, the angle estimate can be significantly improved over that of a single frequency. The second method is referred to as difference beam phase toggling. By flipping the difference beam phase by 180° for two subsequent pulses, the return from a reflected path can be made to cancel.

20 Distribution/Availability of Abstract _X_ unclassified/unlimited __ same as report __ DTIC users	21 Abstract Security Classification Unclassified	
22a Name of Responsible Individuals Professor David C. Jenn	22b Telephone (include Area Code) 408-656-2254	22c Office Symbol EC/JN

DD FORM 1473,84 MAR   83 APR edition may be used until exhausted   security classification of this page

All other editions are obsolete   Unclassified

Methods for Improving Low-Angle, Low-Altitude
Radar Tracking Accuracy

by

Ali Ozkara
Lieutenant Junior Grade, Turkish Navy
B.S., Turkish Naval Academy, 1987

Submitted in partial fulfillment
of the requirements for the degree of

MASTER OF SCIENCE IN SYSTEMS ENGINEERING

from the

NAVAL POSTGRADUATE SCHOOL
September 1993
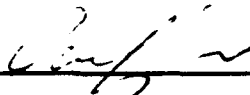
Author: _____
Ali Ozkara

Approved by: _____
David C. Jenn, Thesis Advisor
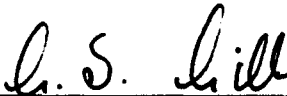
_____
Gurnam Gill, Second Reader
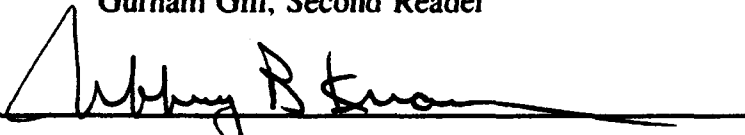
_____
Jeffrey B. Knorr, Chairman
Electronic Warfare Academic Group

ABSTRACT

This thesis studies the problem of low-angle, low-altitude target tracking where the presence of multipath causes large angle errors. The problem is examined for a low sidelobe monopulse radar over a flat earth. A detailed multipath model is used to simulate the reflecting surface and the reflected signal is included in the monopulse processing simulation. Using this model the tracking error is obtained, and two multipath error reduction techniques are evaluated. The first method uses frequency agility to measure the angle over a wide frequency range. By averaging the results of many frequencies, the angle estimate can be significantly improved over that of a single frequency. The second method is referred to as difference beam phase toggling. By flipping the difference beam phase by 180° for two subsequent pulses, the return from a reflected path can be made to cancel.

DTIC QUALITY INSPECTED 8

Accesion For		
NTIS CRA&I	☑	
DTIC TAB	☐	
Unannounced	☐	
Justification		
By		
Distribution /		
Availability Codes		
Dist	Avail and / or Special	
A-1		

iii

TABLE OF CONTENTS

ACKNOWLEDGEMENTS

I. INTRODUCTION

At low elevation angles radar systems can make large errors in angular measurements because a signal reflected from the surface of the earth (ground or sea) enters within the main beam response of the antenna. The reflected electromagnetic (EM) signal adds to the direct signal coming from the target, and the response to the total signal no longer represents the actual target position. This general problem is referred to as multipath tracking error.

The problem of multipath propagation is closely related to multiple-target resolution. In order to make accurate measurements of a target's position, the desired target must be resolved from the image, from the other targets, and from the surrounding clutter which might mask the desired signal or interfere with the measurement process. In modern radar systems difference in any of the radar coordinates (range, angle and Doppler frequency) is sufficient to permit resolution of a target. In general, target signals are received by two or more paths, one of which is the direct path and the other via reflection or diffraction from surfaces surrounding the radar. The surface reflected target signals have approximately the same azimuth, range, and Doppler frequency as the direct signal, and hence can be resolved only in elevation angle. The problem becomes critical when the target is at low elevation angle (on the order of the radar beamwidth, or less), in which case the reflections enter the main beam along with the direct signal. If the elevation angle of the target is relatively small with respect to the beamwidth of the antenna, both

1

signals are summed in the antenna and the location of the target can no longer be accurately determined. At high elevation angles the reflected signals enter the sidelobes of the antenna and thus are usually attenuated sufficiently so that the reflected signal is not a significant part of the total antenna response.

The purpose of this thesis is to evaluate several solutions to the low-angle tracking problem where conventional tracking radars encounter difficulty due to the presence of multipath. The two methods considered are frequency agility and difference beam phase toggling. Frequency agility eliminates multipath errors by operating over a wide frequency range. Since the interference between the direct and reflected signal is frequency dependent, they add constructively at some frequencies and destructively at others. The change in frequency provides enough information to correct for multipath errors. The disadvantage is that the radar receiver and signal processing is more complicated than in the usual single channel narrowband radar.

Difference beam phase toggling is a new method that essentially compares the target return from two successive pulses. However, the difference channel phase is flipped 180° for the second pulse. Assuming that the target parameters are approximately the same for both pulses, and that the antenna is pointed close to the target, the difference channel signal will only contain the main target return, while the multipath components cancel. It was found that the beam pointing error could be reduced by approximating 1/2 in most operational scenarios. Furthermore, it is an easy signal processing upgrade for most monopulse radars.

2

Chapter II discusses the multipath problem and derives the reflection formulas for a flat earth. Chapter III describes the monopulse antenna operation and two different antenna amplitude distributions are simulated. In Chapter IV the monopulse processor is defined and the tracking error is calculated. Chapter V covers the two error correction methods which are frequency agility and difference beam phase toggling. Chapter VI includes conclusions and recommendations.

II. GROUND EFFECTS-MULTIPATH

A. INTRODUCTION

The propagation of radar waves is affected by the earth's surface and its atmosphere. Complete analysis or prediction of radar performance must take into account propagation phenomena since most radars do not operate in isolated free space. For radar detection calculations, the free space restriction can be removed by including the effects of reflections from the surface of the earth, refraction or bending of radar beams caused by traveling through the atmosphere, and the attenuation or absorption of electromagnetic energy by atmospheric gases. The quantative results can be obtained only by simplifying assumptions and incorporating the results of a vast amount of experimentally measured parameters. In addition to atmospheric effects, meteorological conditions such as rain, fog and clouds can also effect the propagation of radar waves. These effects can be quantatively calculated and incorporated in radar detection calculations.

The earth surface, either land or sea, is present in most radar applications. The ground effects on radar signals can be divided into two major categories: (1) multipath effects and (2) clutter. The earth surface patch affecting forward propagation is usually found between the radar and the target, and the presence of the surface adds more paths for the radar signal. When the surface provides additional targets, it is referred to as clutter. For multipath, the ground's relevant quality is its forward-scattering properties. As clutter, its backscattering properties are important.

Excluding the case of perpendicular incidence, a smooth mirror-like surface provides strong forward scattering and weak backscattering. On the other hand, a rough surface is a good backscatterer and relatively poor forward scatterer.

B. REFLECTION COEFFICIENT OF THE EARTH

Three factors effect the earth reflection coefficient: (a) the reflection coefficient of the earth surface, assuming it is perfectly smooth and flat; (b) the surface roughness; and (c) the divergence due to the earth surface curvature. For low-altitude applications the earth can be considered flat.

In studying the propagation of radio waves at low-elevation angles over the surface of the earth it is necessary to take into account forward scattering. When a wave encounters a smooth plane surface which is very large in extent compared with a wavelength, specular reflection takes place, and the angles of incidence and reflection are equal (Snell's law). The reflection coefficient is defined as the ratio of the amplitude of the reflected wave to the amplitude of the incident wave. The reflection coefficient of a smooth earth is determined using Fresnel's equations for the reflection of a plane wave from a smooth dielectric surface [Ref 1]. These classical formulas give the reflection coefficients for horizontal and vertical polarization as a function of electrical properties of the ground composition. The relevant properties of matter are specified by a complex number, the relative dielectric constant ε, which is the ratio of the dielectric constant of the material to the dielectric constant of a vacuum. The reflection coefficient Γ is a function of the complex dielectric constant of the surface, as well as the frequency,

5

polarization, and depression angle of the wave. The complex dielectric constant ε is itself a function of the frequency, as well as the permitivity K and conductivity σ of the surface

$$\varepsilon = \varepsilon' - j\varepsilon'' \approx \frac{K}{\varepsilon_0} - j60\lambda\sigma \qquad (2.1)$$

where ε_0 is the dielectric constant of free space, λ is the signal wavelength in meters, and σ is the conductivity in Siemens per meter.

Fresnel's equations for horizontal and vertical polarization yield the corresponding reflection coefficients

$$\Gamma_H = \frac{\sin\alpha - \sqrt{\varepsilon - \cos^2\alpha}}{\sin\alpha + \sqrt{\varepsilon - \cos^2\alpha}} \qquad (2.2)$$

$$\Gamma_V = \frac{\varepsilon\sin\alpha - \sqrt{\varepsilon - \cos^2\alpha}}{\varepsilon\sin\alpha + \sqrt{\varepsilon - \cos^2\alpha}} \qquad (2.3)$$

Horizontal and vertical are defined with respect to the earth's surface when α is small as shown in Figure 2.1. The grazing angle α is measured from the surface to the incident ray path. Note that since ε is complex, so is Γ. In its polar representation Γ is given by magnitude ρ and phase ϕ. Thus

$$\Gamma_H = \rho_H e^{-j\phi_H}, \qquad \Gamma_V = \rho_V e^{-j\phi_V} \qquad (2.4)$$

6
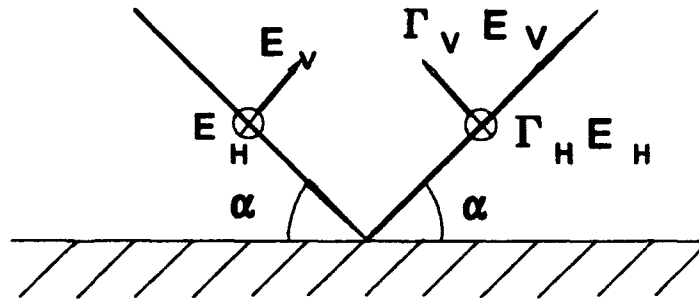
Figure 2.1 Definition of Vertical and Horizontal Polarizations.

Plots of the magnitude and the phase of the reflection coefficient for $\varepsilon'=69$ and $\varepsilon''=39$, calculated using (2.2) and (2.3), are given in Figures 2.2 and 2.3. These values of ε' and ε'' are typical for seawater at 20-25 ^{0} C and for an electromagnetic wavelength of 0.1 m. As the figures show, at very small grazing angles, both reflection coefficients approach -1; that is,

$$\Gamma_H = \Gamma_V = -1, \qquad \alpha = 0^\circ \qquad (2.5)$$

The general behavior of ρ_V and ρ_H seen in Figure 2.2 is typical of other wavelengths and surfaces. Horizontal polarization maintains a reflection coefficient magnitude of approximately one at all depression angles, whereas a vertically polarized

field is more poorly reflected at small to medium angles of depression (around the Brewster angle). In other words, a vertically polarized wave is less susceptible to ground multipath.
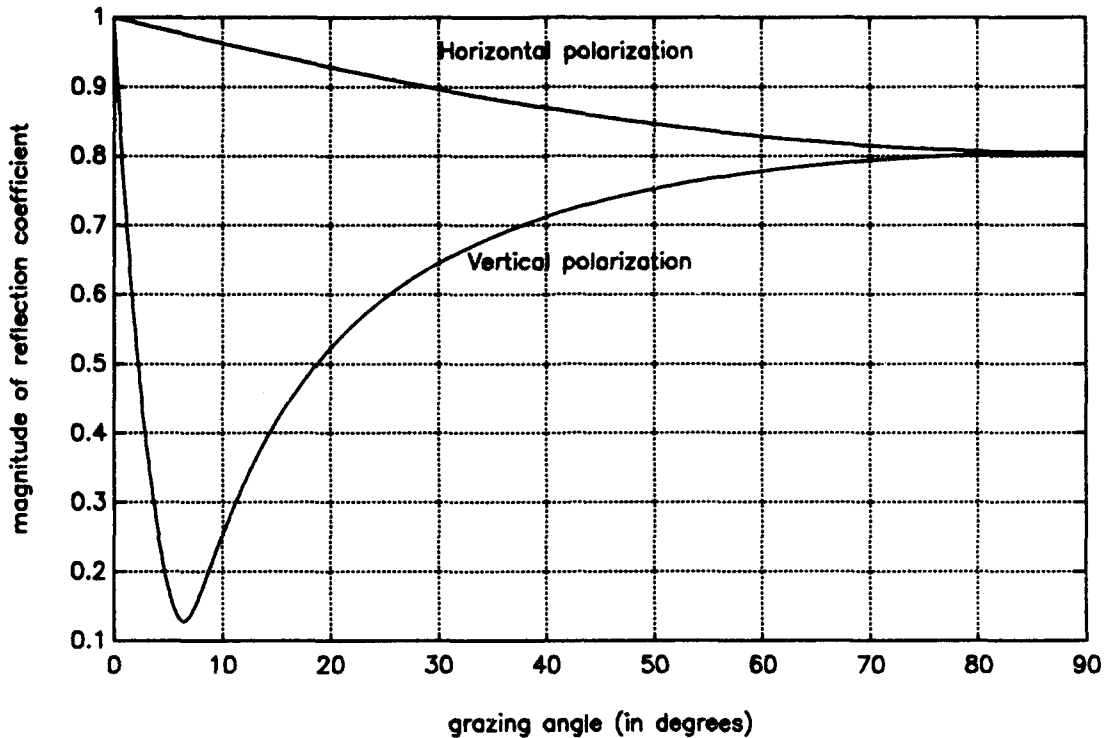
Figure 2.2 The Magnitude of the Reflection Coefficients for ε'=69, ε''=39.

To summarize the characteristics of the reflected waves as illustrated in Figures 2.2 and 2.3:

(a) The magnitude of the reflection coefficient for horizontal polarization ρ_H has the value 1 at very small grazing angles and decreases monotonically as the grazing angle α increases.

8

(b) The coefficient for vertical polarization on the other hand has a single, well-defined minimum, which is $\rho_v = 0$ provided $\sigma = 0$.
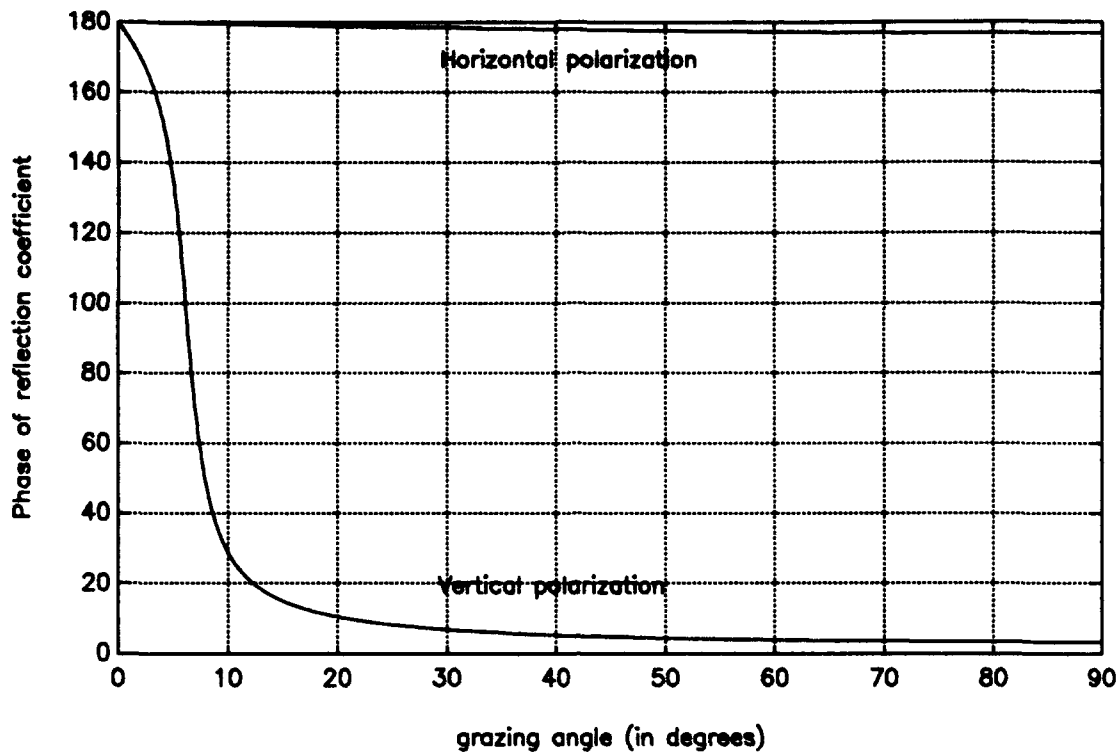
**Figure 2.3** The Phase of the Reflection Coefficients for $\varepsilon' = 69$, $\varepsilon'' = 39$.

(c) At normal incidence (grazing angle $90°$) the reflection coefficients for horizontal and vertical polarization are equal; the Fresnel equations reduce to

$$\Gamma = \frac{1 - \sqrt{\varepsilon}}{1 + \sqrt{\varepsilon}} \qquad (2.6)$$

in this case.

9

(d) For horizontal polarization the phase lag ϕ_H is nearly π for all values of α, but for vertical polarization the phase lag ϕ_V goes from π at small grazing angles ($\alpha \leq 8°$) to zero for large grazing angles ($\alpha \leq 45°$) with the changeover around Brewster's angle.

(e) For very low grazing angles in the neighborhood of $1°$ or less ρ_V and ρ_H are nearly one and ϕ_V and ϕ_H are nearly π. As a result, there should be little difference in the propagation of horizontally and vertically polarized waves over the ground at very low angles.

C.   MULTIPATH

Multipath is defined as the propagation of a wave from one point to another by more than one path. When multipath occurs in radar, it usually consists of a direct path and one or more indirect paths by reflection from the surface of the earth or sea or from large man-made structures. At frequencies below 40 MHz it may also include more than one path through the ionosphere.

If the reflection surface is flat or smoothly rounded, the multipath is specular (mirror-like); if the surface is irregular, the multipath is diffuse. When the mean contour of the surface is smooth but the surface is perturbed by small-scale irregularities, both specular and diffuse components (also called the coherent and incoherent components respectively) are present.

For low-angle targets over a reflecting surface, there is not enough separation in angle, range, or Doppler to resolve the direct and reflected waves. Specular multipath is equivalent to the special case of unresolved targets. In the case of multipath, however, the

10

targets are not independent but related according to the geometry and electrical characteristics of the reflecting surface.

Specular multipath causes erratic elevation tracking at low target elevations within a beamwidth of the horizon, and causes a significant elevation error even at target elevations a few beamwidths above the horizon. The effects are deterministic in the sense that if the pertinent radar characteristics, reflection surface characteristics, and multipath geometry are specified, the results can be computed. The results can also be expressed statistically if they are to apply to a specified range of conditions or if the parameters cannot be specified exactly.

Diffuse multipath effects are somewhat noise-like and can be treated only statistically, since they are caused by irregularities over the entire surface, the exact contour of which is unknown and can vary unpredictably with time (as in the case of waves on water or wind-swept vegetation on land) .

1. Flat-earth specular multipath model

Consider specular reflection from the surface of the earth or sea, with the limitation that the surface is flat and horizontal. The following assumptions have been made for deriving a specular multipath model for the earth:

(a) The ground reflectivity remains nearly constant over the reflecting region for the range of elevation angles considered.

(b) Specular reflection occurs, which implies that the Rayleigh criterion must be satisfied [Ref. 2].

(c) The target range and the height are much greater than the receiving-antenna height.

The specular reflection problem is approached by first considering the geometry of a flat reflecting plane as in Figure 2.4.
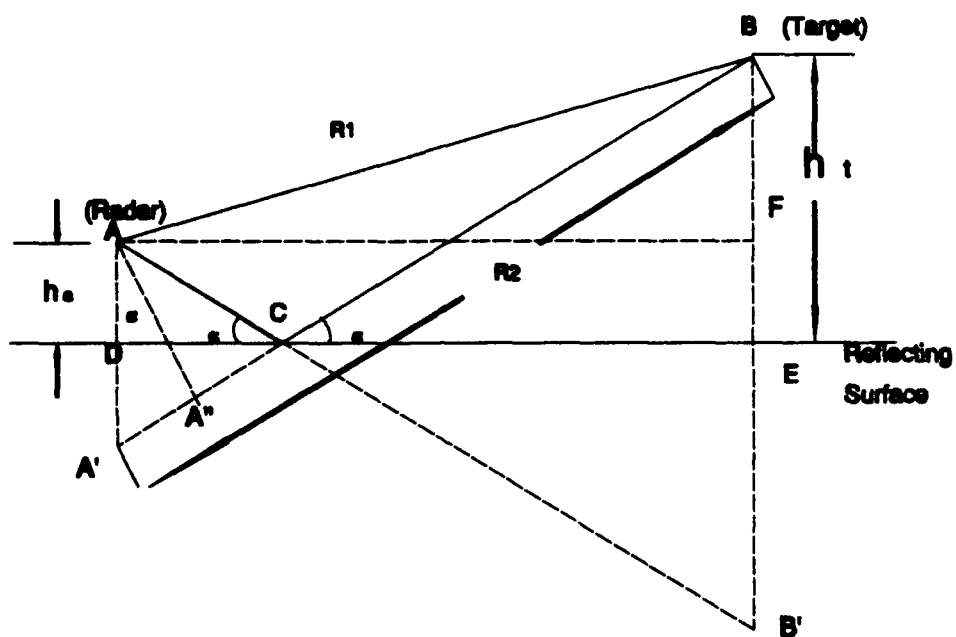
Figure 2.4 Geometry of Earth's Specular Reflection Model.

Point A is the location of a ship-based or ground-based radar (source) is at a height h_a above the earth's surface. The target is at height h_t and located at B. The direct path AB has length R_1 and the reflected path ACB has length R_2. The angle α is

the grazing angle of the reflected ray at the reflection point. The reflected path length R_2 is given by:

$$R_2 = \frac{(h_t + h_a)}{\sin\alpha} \tag{2.7}$$

The grazing angle α is computed as follows. The lengths AF and DE are equal and given by

$$(AF)^2 = R_1^2 - (h_t - h_a)^2$$

$$(DE)^2 = (DC + CE)^2 \tag{2.8}$$

$$= \frac{(h_t + h_a)}{\tan\alpha}$$

Equating AF and DE gives

$$\tan\alpha = \sqrt{\frac{(h_t + h_a)}{R_1^2 - (h_t - h_a)^2}} \tag{2.9}$$

Using the value of α from Equation (2.9) the indirect path length R_2 can be determined. The ground reflectivity coefficient may be represented by the complex function

$$\Gamma = \rho e^{-j\phi} \tag{2.10}$$

where as defined above ρ is the change in the amplitude and ϕ is the change in the phase angle of the reflected energy. The phase difference of the signals arriving at the target

13

through the reflected and direct paths will be proportional to the difference of path lengths R_2 and R_1:

$$\phi_d = \frac{2\pi}{\lambda}(R_2 - R_1) \tag{2.11}$$

where ϕ_d represents the phase difference due to the pathlength difference between direct and indirect signals. To find the resulting phase difference, the reflection phase in Equation (2.10) must be added to the path difference phase,

$$\phi_T = \phi + \phi_d \tag{2.12}$$

where ϕ_T is the total phase shift.

The target radiates or reflects signals in all directions, and the radar receives a direct signal from an elevation angle α_t plus a reflected signal from angle α_r. If the antenna voltage gain pattern is $f(\theta)$, the total signal received is

$$E = A_t f(\theta_B) + A_r \rho_0 f(\theta_C) e^{-j\phi_T} \tag{2.13}$$

The factors A_t and A_r (usually assumed equal) represent the free-space field strengths of the target signal at the antenna and image antenna. The angle θ_B and θ_C are the antenna angles, in the directions of points B and C in Figure 2.4, and ρ_0 is the reflection coefficient for the flat surface at grazing angle α [Ref. 3].

2. Effect on detection

In addition to its effect on angle measurement, multipath has a well-known effect on detection. In tracking radars an elevation pattern typically has a beamwidth of

14

a few degrees at most (less than one degree in some cases). The multipath lobing pattern results due to interference between the direct and reflected waves, which are alternatively in phase and out of phase as the elevation varies. The ratio of free-space beamwidth to the multipath lobe spacing (that is, the number of lobes within the free-space beamwidth) is approximately equal to twice the height of the center of the antenna above the reflecting surface divided by the diameter (or vertical dimension) of the antenna.

The difference pattern of a monopulse antenna also has an interference lobing structure due to multipath. This affects elevation angle measurements but does not affect detection. In this study the effect of multipath on detection is not a primary interest.

15

III. MONOPULSE OPERATION AND ANTENNA SIMULATION

A. INTRODUCTION

The concept of monopulse emerged from the earlier concept of direction finding by simultaneous lobing. When an incoming wave from an isolated pulsed source at sufficiently great range is received on two different antenna patterns simultaneously, the absolute amplitudes and absolute phases of the received signals may vary with the changing characteristics of the source or of the propagation medium, but their relative values are functions only of the angle of arrival. By focusing attention on the ratio of pattern functions rather than on the pattern functions themselves, all of the parameters except angle of arrival are removed, in principle. The instantaneous formation of this ratio upon reception of each pulse to obtain the angle of arrival of radiation from all sources within the beam independently of their absolute amplitude levels is one of the two distinguishing characteristics of the monopulse concept. The other is symmetry of the angle output about the boresight axis.

1. Monopulse operation

In its simplest form the concept of monopulse involves a comparison of just a single pair of signals, which in general may be complex. This is sufficient to determine angle of arrival in a single plane, e.g., azimuth or elevation. Complete three -dimensional tracking, however, requires angle of arrival measurements in two orthogonal planes.

16

Therefore nearly all tracking systems in use involve comparison of two pairs of signals, usually one pair in azimuth and the other in elevation [Ref. 4].

In contrast to conical-scanning radar, in which the beam scans on both transmission and reception, the angle of arrival measured by a monopulse radar is determined solely by its receiving characteristics. Transmission remains the same as for any conventional pulse radar. This gives monopulse radar some other distinct advantages in addition to that of instantaneous precision direction finding, among them being the absence of any telltale scanning modulation and an increase in transmitted power in the boresight direction.

In practice the angle of arrival determined by application of the concept of monopulse can never be measured instantaneously since there will always be some averaging present. In any practical system the time constant of the system can never quite be reduced to zero. In some cases smoothing may be introduced deliberately in order to remove the random fluctuations in angle of arrival caused by glint.

The monopulse concept generally is applied in one of two ways, regardless of whether it is used to sense the direction of an active or of a passive radiating source. In one way the output of the system is taken directly as a measure of the angle of arrival of the incoming wave relative to the boresight direction, while in the other it is limited solely to an indication of the boresight direction itself. The latter application, boresighting, was the first to be developed because it is the simplest, and since it is also the most common it is sometimes mistaken to be the only application. It was developed originally for automatic precision target tracking. Once the target has been acquired, it can be

17

isolated from other targets and tracked in range by gating its return, after which it can be tracked in angle by driving the antenna from the angle output of the radar in a closed servo loop.

Existence of a well-defined angle of arrival is implied in the concept of monopulse by the assumption that the pulsed source is isolated in space at a sufficiently great range. In the presence of a number of isolated pulsed sources the angle of arrival from each will still be well defined, provided no two are received simultaneously. Pulses received simultaneously from two similar sources cannot be separated; hence the measured angle of arrival does not represent the direction of either source.

2.   Amplitude-comparison monopulse

This is a form of monopulse employing receiving beams with different amplitude-versus-angle patterns. If the beams have a common phase center, the monopulse is pure amplitude-comparison; otherwise, it is a combination of amplitude-comparison and phase-comparison.

The amplitude-comparison monopulse employs two overlapping antenna patterns to obtain the angular error in one coordinate. The two overlapping antenna beams may be generated with a single reflector or with a lens antenna illuminated by two adjac nt feeds or an array antenna. The sum and difference of the two antenna patterns are shown in Figure 3.1. The sum pattern is used for transmission, while both the sum pattern and the difference pattern are used on reception. The signal received with the difference pattern provides the magnitude of the angle error. The sum signal provides the range measurement and is also used as a reference to extract the sign of the error signal.

18

Signals received from the sum and the difference patterns are amplified separately and combined in phase-sensitive detector to produce the error signal [Ref. 5].
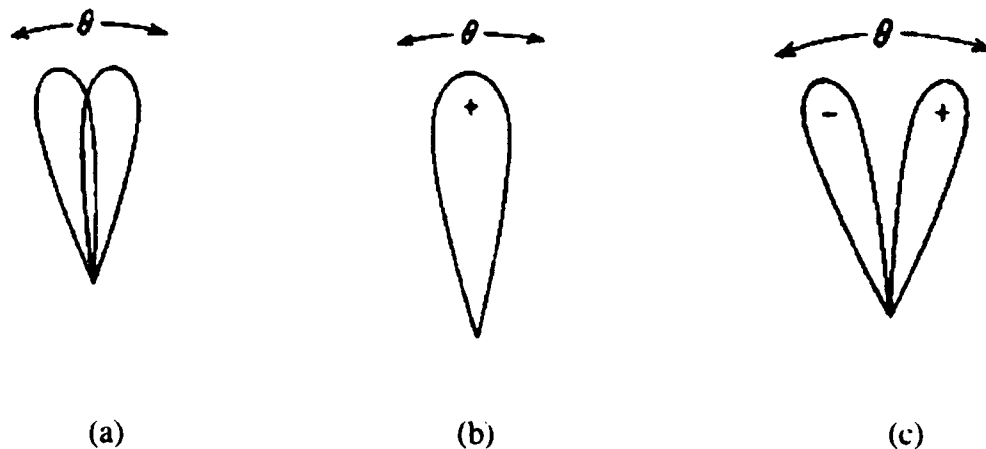
Figure 3.1 Monopulse Antenna Patterns. (a) Overlapping Antenna Patterns; (b) Sum Pattern; (c) Difference Pattern.

3. Monopulse array antennas

In particular, monopulse has been implemented in various ways in array antennas. One approach is to partition the array into smaller arrays (subarray) by dividing the array into four quadrants. Within each quadrant the outputs of the individual elements are summed to form a single output of the quadrant.

It is also possible to combine the element outputs in such a way as to produce simultaneous squinted beams, each with an identifiable output point in the system, from which the sum and the differences can be obtained in the same way as in a reflector antenna. Such an arrangement would be a clear case of amplitude-comparison.

19

Most arrays do not conform to these simple models. Usually the outputs of the elements are combined in beamformers, which are networks of connections, with appropriate amplitude and phase weighting, to produce the sum and difference voltages directly. In such cases there are no points in the system at which the voltages can be identified as the outputs of a set of sequinted beams or of a set of parallel beams with different phase centers. Nor is there anything about the shape of the sum and difference patterns that identifies as array as amplitude-comparison or phase-comparison.

A voltage pattern of an antenna is approximately equal to the Fourier transform of an aperture illumination function from which it was produced. In a mechanically steered reflector antenna or lens antenna the illumination function is determined by the design of the feed, the f/D ratio, and any power dividers, combiners, or hybrids used in forming the pattern. The same is true of certain types of array antennas which act as reflectors or lenses, except that they permit electronic rather than mechanical steering (reflect-arrays).

In most array antennas, however, the illumination function is formed directly in the aperture plane by control of the amplitudes and phases of the excitation coefficients of the individual radiating elements of the array. The elements are usually a set of identical radiators such as dipoles, open ended waveguides, slots in waveguides, or horns. For reasons of economy or design simplification, with some sacrifice in performance, the elements are often grouped into subarrays. The amplitude is uniform within each subarray but differs from one subarray to the next.

The pattern direction is steered by imposing an appropriate linear phase progression from element to element along the aperture in the desired direction. The element amplitudes are set at values that will produce the illuminating function for the desired pattern shape. In the past, electromechanical scanners have been used to achieve variable phase tapers, but modern array antennas use electronic steering for rapid and agile beam scanning.

Two simultaneous receiving patterns (a sum and a difference) are needed for monopulse in a single angular coordinate, and three (a sum and two differences) are needed for two-coordinate monopulse. The sum and difference patterns (as well as the transmitting pattern) are all steered in the same direction and therefore they use the same settings of the element phases, but different amplitude weights.

The main advantage of array antennas is their ability to change beam direction rapidly without inertia. The principal disadvantages are complexity and cost [Ref. 6].

B.   SUM AND DIFFERENCE BEAM ANTENNA DISTRIBUTIONS

A typical monopulse antenna diagram is shown in Figure 3.2. Sum and difference beams are formed simultaneously using a common array aperture. The complexity of the beamforming networks depends on the requirements imposed on the pattern characteristics.

1. Sum and difference beams from uniform arrays

An array of identical elements of uniform magnitude can also be used to generate sum and difference beams. The array factor can be obtained by considering the elements to be point sources where

$$AF = \sum_{n=1}^{N} e^{j(n-1)(kd\cos\theta + \beta_n)} \tag{3.1}$$

where

$$\beta_n = \begin{cases} 0 & \text{all } n \text{ for sum beam} \\ 0 & n \leq \dfrac{N}{2} \text{ difference beam} \\ \pi & n > \dfrac{N}{2} \text{ difference beam} \end{cases} \tag{3.2}$$

A MATLAB program to generate sum and difference beams is included in Appendix A. Typical sum and difference patterns are shown in Figures 3.3 and 3.4.

22
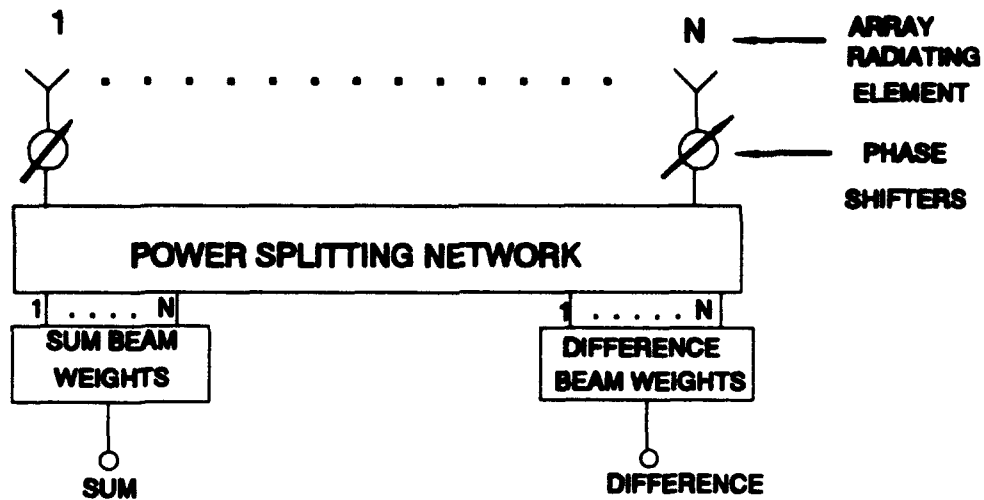
Figure 3.2 A Typical Monopulse Antenna Diagram.

The disadvantage of uniform array weighting is evident from the pattern. In both sum and difference cases the sidelobe levels are unacceptablely high. There is no single amplitude distribution that provides low sidelobes for both the sum and difference beams simultaneously. Independent control of the two beams is required, i.e. separate feed networks must be used for the two channels. This complicates the antenna design and increases the cost, but it is a necessity for accurate anti-jam tracking.

The chosen low sidelobe distributions for the sum and difference beams are Taylor and Bayliss, respectively. The characteristics of these two functions are described briefly in the following sections.
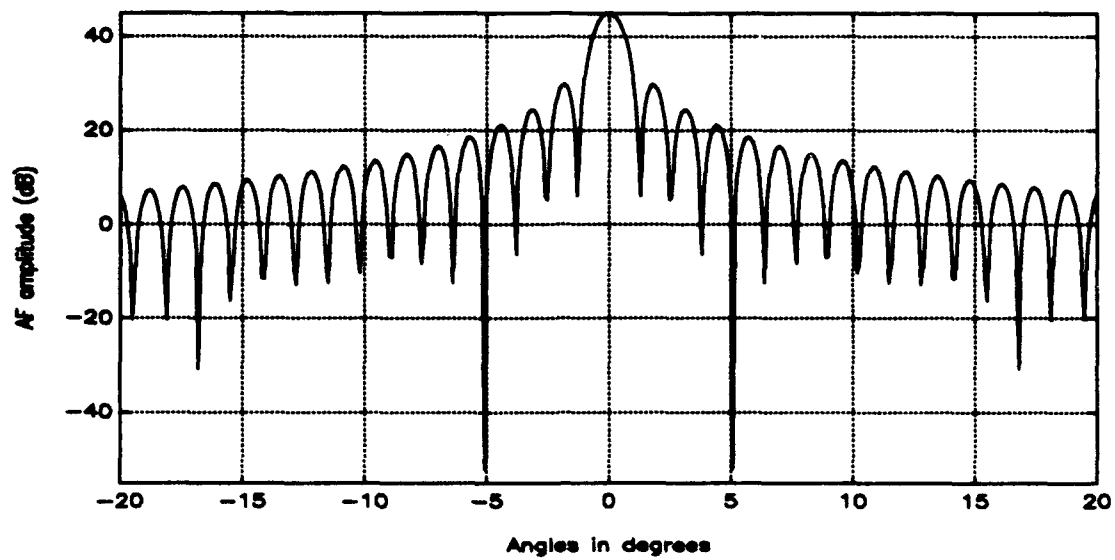
Figure 3.3 Uniform Distribution Sum Pattern for a 90 Element Array with d=0.5λ.
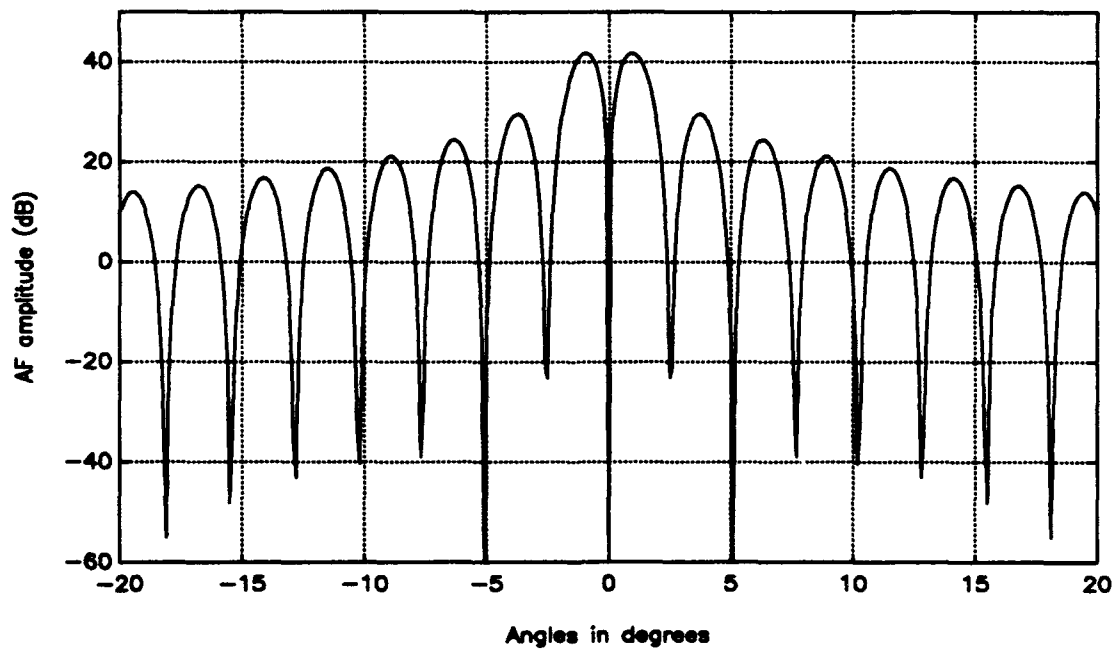
Figure 3.4 Uniform Distribution Difference Pattern for a 90 Element Array with d=0.5λ.

24

2. Taylor amplitude distribution

The Taylor design [Ref. 7] yields a pattern that displays an optimum compromise between beamwidth and sidelobe level. Taylor leads to a pattern whose first few minor lobes are maintained at equal and specific level while the remaining lobes decay monotonically. The design is for far-field patterns, and it is based on a line-source distribution symmetrical about the array center.

Ideally the normalized space factor that yields a pattern with equal-ripple minor lobes is given by

$$SF(\theta) = \frac{\cosh\left[\sqrt{(\pi A)^2 - u^2}\right]}{\cosh(\pi A)} \tag{3.3}$$

which has a maximum value when $u=0$. For a continuous line source of length l located along z axis

$$u = \pi \frac{l}{\lambda} \cos\theta \tag{3.4}$$

In (3.3) A is a constant which is related to the maximum desired sidelobe level R_0 by

$$\cosh(\pi A) = R_0 \ (voltage\ ratio) \tag{3.5}$$

Since (3.3) is ideal and cannot be realized physically, Taylor suggested that it be approximated (within a certain error) by a space factor comprised of a product of factors whose roots are the zeros of the pattern. Because of its approximation to the ideal Tschebyscheff design, it is also referred to as *Tschebyscheff error*. The Taylor space factor is given by

25

$$SF(u, A, \bar{n}) = \frac{\sin(u)}{u} \frac{\prod_{n=1}^{\bar{n}-1}\left[1-\left(\frac{u}{u_n}\right)^2\right]}{\prod_{n=1}^{\bar{n}-1}\left[1-\left(\frac{u}{n\pi}\right)^2\right]} \tag{3.6}$$

$$u = \pi v = \pi\frac{l}{\lambda}\cos\theta \tag{3.7}$$

$$u_n = \pi v_n = \pi\frac{l}{\lambda}\cos\theta_n \tag{3.8}$$

where θ_n represents the locations of the nulls. The parameter $\bar{n}$ is a constant chosen by the designer so that the minor lobes for $|v|=|u/\pi|\leq \bar{n}$ are maintained at a nearly constant voltage level of $1/R_0$; for $|v|=|u/\pi|> \bar{n}$ the envelope, through the maxima of the remaining minor lobes, decay at a rate of $1/v=\pi/u$. In addition, the nulls of the pattern for $|v|\geq\bar{n}$ occur at integer values of v.

In general, there are $\bar{n}-1$ inner nulls for $|v|<\bar{n}$ and an infinite number of outer nulls for $|v|\geq\bar{n}$. To provide a smooth transition between the inner and the outer nulls, Taylor introduced a parameter σ. It is usually referred to as the scaling factor, and it spaces the inner nulls so that they blend smoothly with the outer ones. In addition, it is the factor by which the beamwidth of the Taylor design is greater than that of the Dolph-Tschebyscheff, and it is given by

26

$$\sigma = \frac{\bar{n}}{\sqrt{A^2 + \left(\bar{n} - \frac{1}{2}\right)^2}}$$ (3.9)

The normalized line-source distribution which will yield the desired pattern is given by

$$I(z') = \frac{1}{l}\left[1 + 2\sum_{p=1}^{\bar{n}-1} SF(p, A, \bar{n}) \cos\left(2\pi p \frac{z'}{l}\right)\right]$$ (3.10)

The coefficients $SF(p, A, \bar{n})$ represent samples of the Taylor pattern, and they can be obtained from (3.4) with u=πp. They can also be found using

$$SF(p, A, \bar{n}) = \frac{[(\bar{n}-1)!]^2}{(\bar{n}-1+p)!\,(\bar{n}-1-p)!} \prod_{m=1}^{\bar{n}-1}\left[1 - \left(\frac{\pi p}{u_m}\right)^2\right] \qquad |p| < \bar{n}$$ (3.11)

while for other values of p, $SF(p, A, \bar{n})=0$. Also $SF(-p, A, \bar{n})=SF(p, A, \bar{n})$.

For an array of discrete elements the appropriate excitation coefficient for element n is usually determined by sampling $I(z)$ at a value of z that corresponds to the element location. For example, if there are N elements with spacing d then $l \approx Nd$ and

$$a_n = I(z')$$ (3.12)

where

$$z'_n = \left[\frac{2n - (N+1)}{2}\right] d$$ (3.13)

This simple sampling approach does not precisely reproduce the Taylor pattern but the difference is negligible as the number of elements increases [Ref. 8].

27

A MATLAB program to generate the Taylor coefficients is given in Appendix B. The pattern for an antenna array of 90 elements for a sidelobe level of 25 dB ($\bar{n}$=5) and element spacing of 0.5λ is shown in the Figure 3.5.
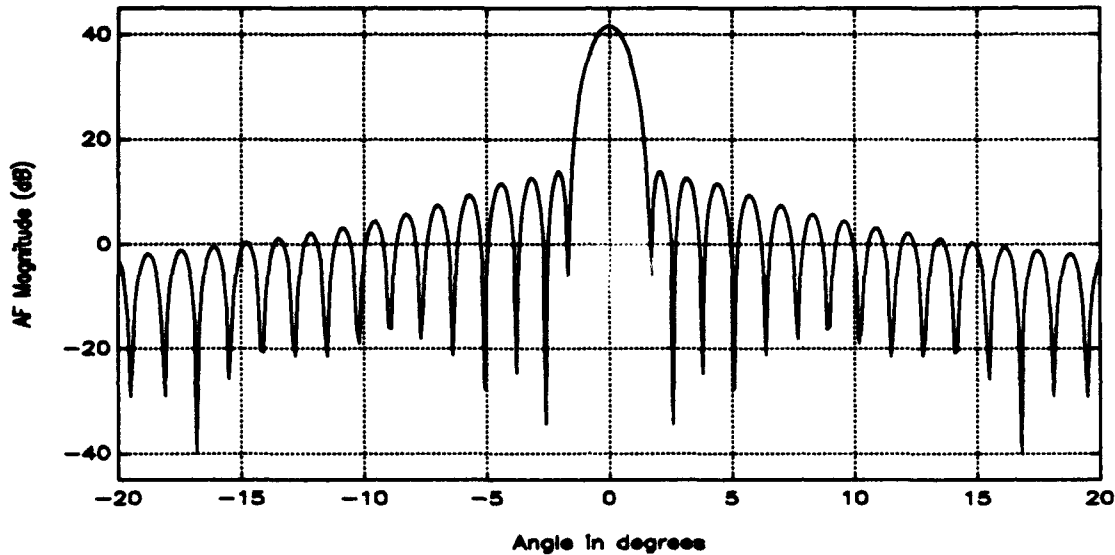
Figure 3.5 Taylor Sum Pattern of a 90 Element Array, d=0.5λ and $\bar{n}$=5.

3. Bayliss amplitude distribution

A low sidelobe symmetric difference beam pattern was developed by E. T. Bayliss [Ref. 8]. Unlike the Taylor space factor, there is no limiting form for the ideal difference pattern. Bayliss performed a parametric study with the aid of the computer, the results of which have yielded the following formulas for root placement:

28

$$u_n = \begin{cases} 0 & n = 0 \\[2mm] \left(\bar{n} + \dfrac{1}{2} \right) \left(\dfrac{z_n^2}{A^2 + \bar{n}^2} \right)^{\frac{1}{2}} & n = 1, 2, 3, 4 \\[4mm] \left(\bar{n} + \dfrac{1}{2} \right) \left(\dfrac{A^2 + n^2}{A^2 + \bar{n}^2} \right)^{\frac{1}{2}} & n = 5, 6, \ldots, \bar{n}-1 \end{cases} \qquad (3.14)$$

The parameters A and z_n are related to the sidelobe level. The aperture distribution for a Bayliss pattern is given by

$$I(z') = e^{-j\beta z} \sum_{m=0}^{\bar{n}-1} SF\left(m + \frac{1}{2} \right) \sin\left[\left(m + \frac{1}{2} \right) \frac{\pi z'}{a} \right] \qquad (3.15)$$

A MATLAB function for the Bayliss coefficients is given in Appendix C. A pattern for an antenna array of 90 elements, for a sidelobe level of 25 dB ($\bar{n}=5$) and element spacing of 0.5λ is shown in the Figure 3.6.
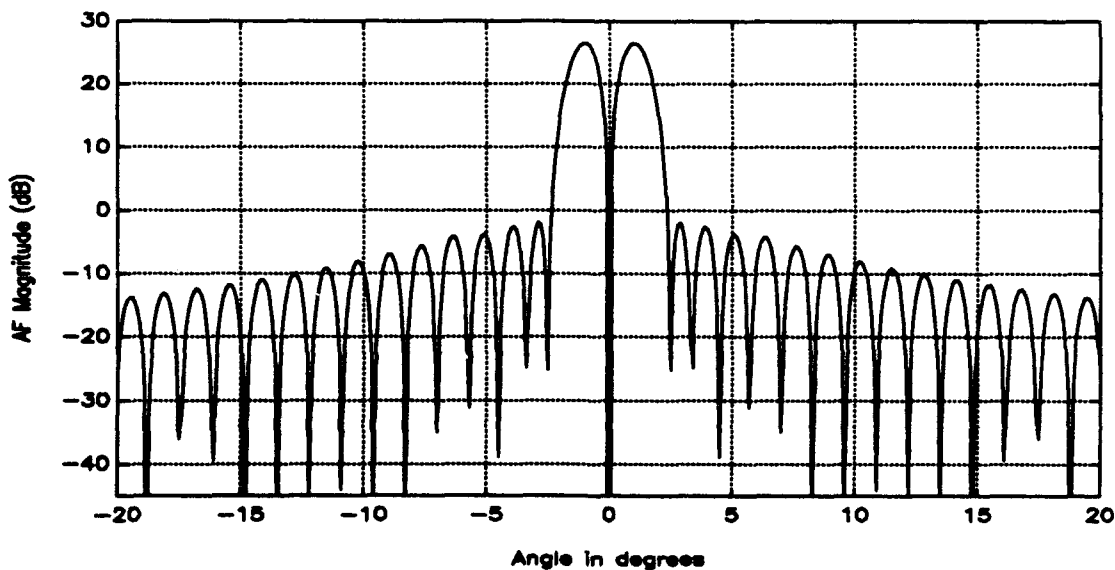
Figure 3.6 Bayliss difference pattern for an array 90 elements, d=0.5λ and ñ=5.

The amplitude distribution is symmetrical about the array center; it is nonzero at the end points, but zero at the midpoint, which is where a phase reversal of 180° takes place.

IV. SIMULATION OF MONOPULSE PROCESSOR AND TRACKING ERROR

A. INTRODUCTION

When the elevation of a target being tracked by a monopulse radar is less than approximately a beamwidth, the radar system sees both the target and its image and tries to null on the composite signal. The radar will then either oscillate about a mean position or oscillate apparently randomly over an angle of about a beamwidth about the horizon. The radar will frequently lose track altogether under these circumstances.

Though multipath can cause significant azimuth tracking error, the errors for typical conditions are mainly in the elevation tracking coordinate, and can be so severe in the low-angle region as to make elevation tracking useless. Unless there is crosstalk in the radar between the azimuth and the elevation tracking channels, errors in azimuth tracking can be neglected and only the elevation channel will be considered from now on.

B. SIMULATION OF MONOPULSE RADAR ERROR PROCESSOR

The monopulse processor is a mechanism used to obtain an estimate of the off-axis angle of the antenna. It can be implemented either with hardware or as a software algorithm on a digital computer. The monopulse radar simulation will consist of: (1) modeling the portions of the system affected by the reflected signal, namely the antenna and receiver; (2) modeling the sea reflection; and (3) calculating the tracking errors caused by the reflected signal. An array antenna of N elements is used and the sum and

31

the difference channel calculations are made separately. Also it is assumed that the channel information is processed digitally so that analog-to-digital conversion is required. The simulation model for the processor is as illustrated in Figure 4.1.
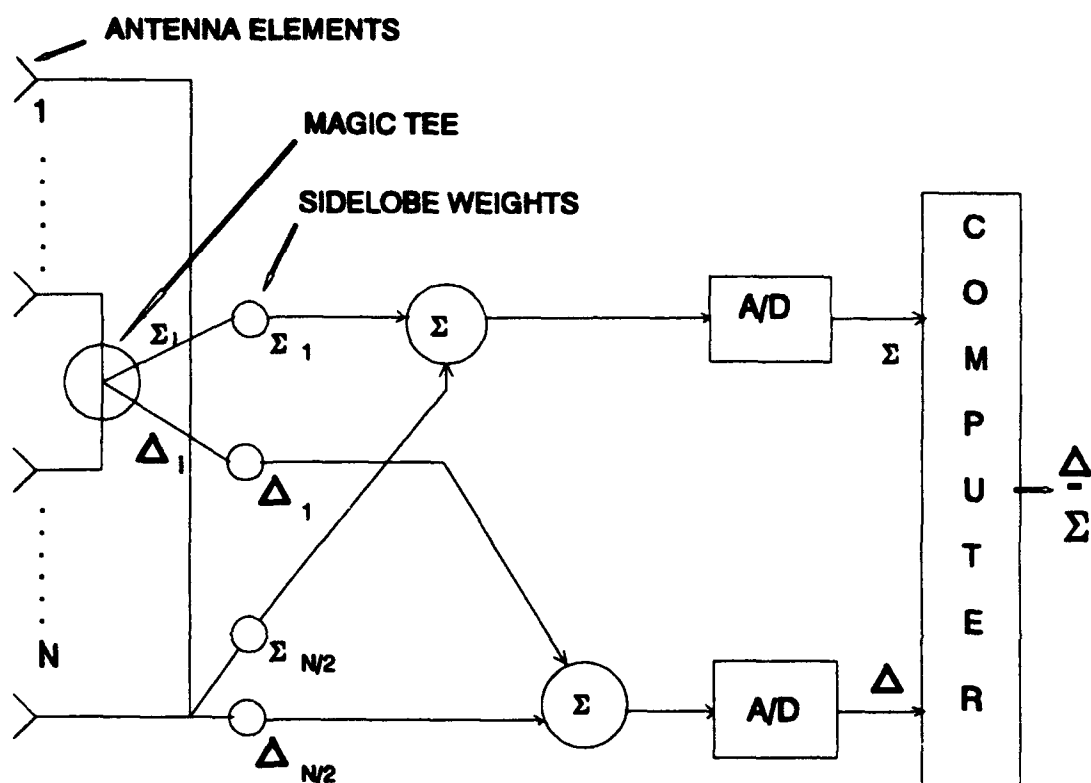
Figure 4.1 Monopulse Processor Simulation Model.

The sea reflection was modeled as a constant reflection coefficient of amplitude 0.9 and a 180 degree phase shift. The earth was considered flat because of the short ranges involved. The magnitude of the coefficient is ρ and the phase α. Figure 4.2 shows the antenna sum and difference patterns and also typical positions of the target and the image on the angle axis. The total sum pattern response is given by the target's value plus the image's value
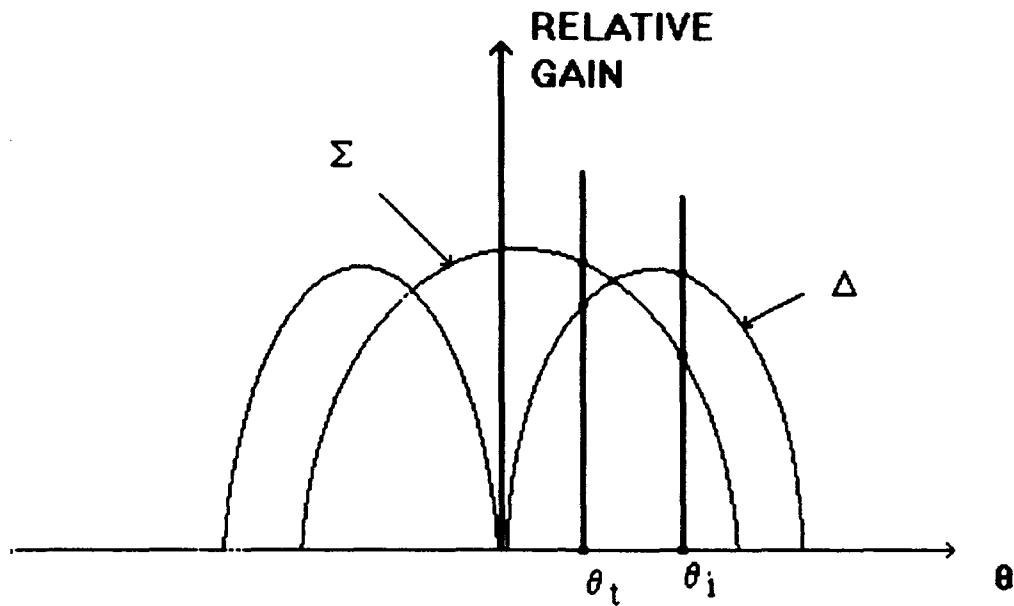
Figure 4.2 The Monopulse Antenna Pattern Pictures Showing Target and Image Responses.

$$\Sigma = \Sigma_t + \rho e^{j\alpha} \Sigma_i \qquad (4\text{-}1)$$

where the subscripts i ant t refer to image and target. Similarly for the difference pattern

response, the target and image responses are summed

$$\Delta = \Delta_t + \rho e^{j\alpha} \Delta_i \qquad (4\text{-}2)$$

The antenna pattern modifies the amplitude and phase of the two incoming vectors. After the antenna effect on the two separate vectors has been computed, the direct and reflected vectors are summed in the antenna. The outputs of the antenna are the vector

33

Σ, representing the sum signal, and a vector Δ, representing the difference signal. The vectors Σ and Δ are processed in the computer and the output is an error signal which in the single target situation would indicate how far the target is off the center of the antenna beam. The error response is calculated using the total difference-to-sum response ratio contributed by target and the reflection

$$e = Re\left\{\frac{\Delta}{\Sigma}\right\} = Re\left\{\frac{\Delta_t + \rho e^{j\alpha} \Delta_i}{\Sigma_t + \rho e^{j\alpha} \Sigma_i}\right\} \qquad (4\text{-}3)$$

The error signal is used in a tracking algorithm that positions the scanning angle to reduce the error signal to some arbitrarily small value. A MATLAB simulation of the error correction algorithm is listed in Appendix D.

Initially the antenna pointing direction is on the target. The low-angle flying target is assumed to be at a constant altitude and the curvature of the earth is neglected. The final position of the beam is taken as the indicated angle of the target, and the difference of this value from the true position of the target is defined as the tracking error.

A typical example of the tracking error that occurs for low sidelobe antennas using Bayliss and Taylor amplitude coefficients is shown in Figure 4.3. The plot illustrates that the error is cyclic, and that the amplitude of the error decreases when the reflected signal enters a difference null. Figure 4.3 shows the error data for a single frequency (9 GHz). At other frequencies similar results are obtained, as shown in Figure 4.4 for 3 GHz, the only difference being that the errors appear to be shifted in range. In other words, the

maxima and minima do not occur at the same range for all frequencies, and this fact can be used to reduce the tracking error.
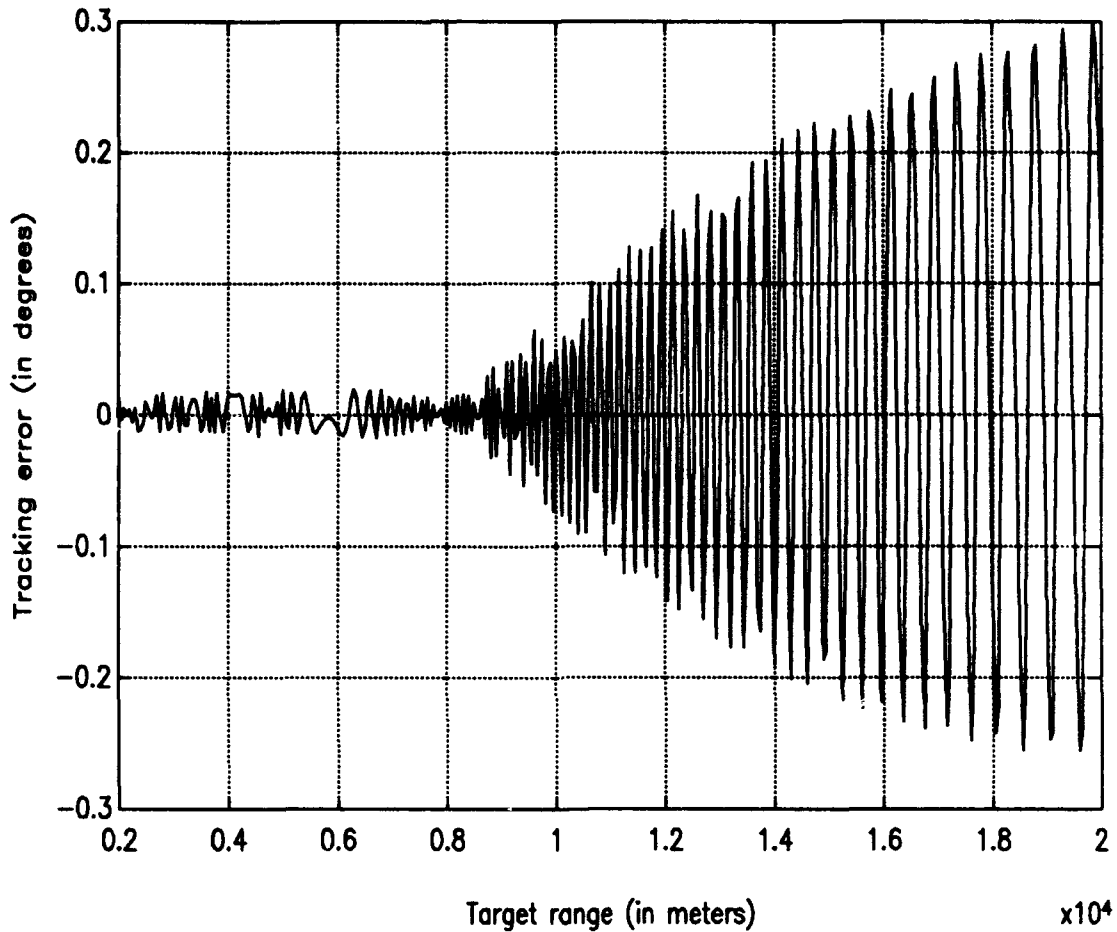
Figure 4.3 Tracking Error Calculated for f=9 GHz, h_2=150 m, h_1=15 m, ρ=0.9, N=90, d=0.5λ. Low Sidelobe Beams.

For the same simulation parameters the tracking error was calculated for an antenna with uniform amplitude coefficients. The results are shown in Figure 4.5 and the program in Appendix E. The period of the error is not changed because both the direct and reflected signal components still enter the antenna through the main beam.

35
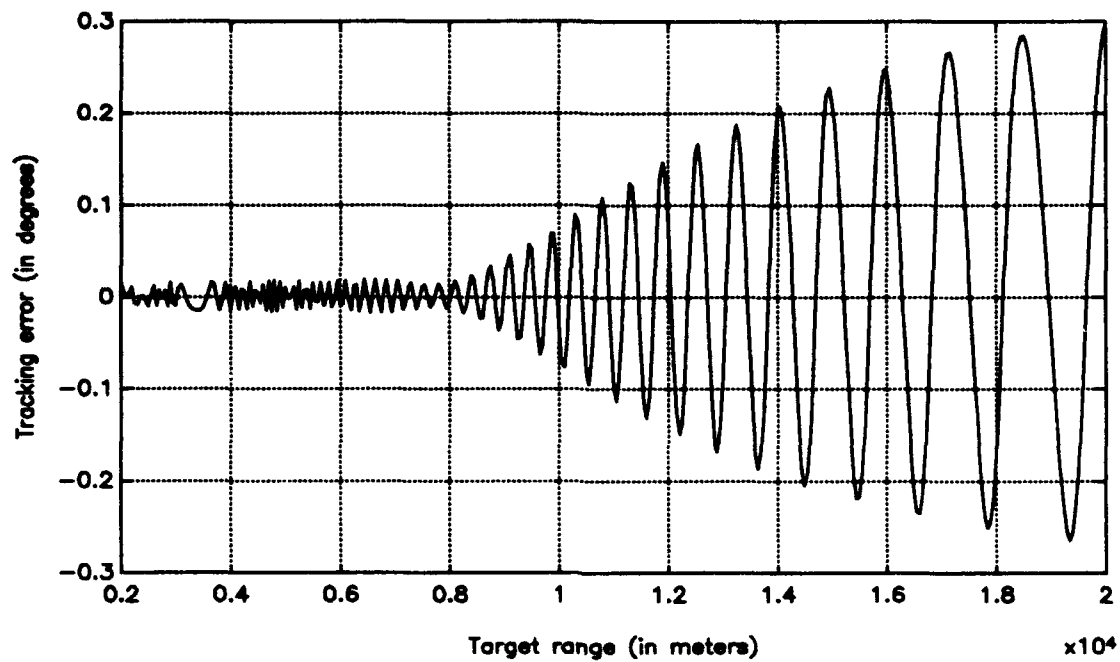
Figure 4.4 Tracking Error Calculated for f=3 GHz, h_2=150 m, h_1=15 m, ρ=0.9, N=90, d=0.5λ. Low Sidelobe Beams.
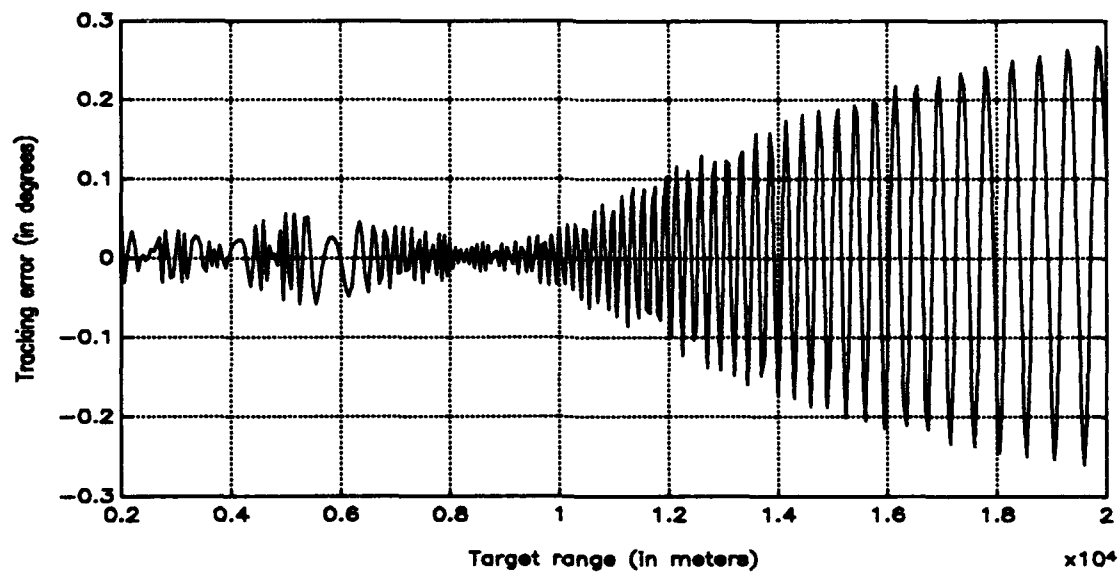
Figure 4.5 Tracking Error Calculated for f=9 GHz, h_2=150 m, h_1=15 m, ρ=0.9, N=90, d=0.5λ. Uniform Amplitude Beams.

V. TECHNIQUES TO REDUCE TRACKING ERROR

A. INTRODUCTION

Resolution in a radar system is defined as the ability to distinguish between closely spaced objects. In the ordinary radar system, the ability to separate and distinguish between objects, or targets as they are called, is provided by two different techniques. The first is dependent on the pulse width of the system and provides resolution in range. The second is dependent on the radiation field pattern and provides angular resolution either in azimuth, elevation, or both.

Here resolution in one plane will be covered, namely, resolution in elevation plane. Such resolution is normally provided by a fan beam having a narrow beam angle in the elevation plane. As the radar antenna beam is swept across a target in space, the reflected signal will generate at the receiver a pattern that corresponds to the antenna radiation pattern; that is to say, the reflected energy will build up to a maximum when a center of the beam falls directly on the target. The energy will decay as the beam passes beyond the target.

In the two target case, when the beam is swept across two targets and as the targets move closer together, it becomes more difficult to distinguish the two until finally they appear as one target. The narrower the radar beam, the closer the targets can come and still be separately distinguishable.

37

The surest way for avoiding tracking error due to multipath reflections via the surface of the earth is to use an antenna with such a narrow beamwidth that it doesn't illuminate the surface. This requires a large antenna or a high frequency. Although such a solution eliminates the problem, there are many practical reasons that preclude the use of the large antenna needed for a narrow bandwidth or against operation at high frequency. High resolution in elevation angle, with adequately low sidelobes, is the basic means used for this in radar, but there are upper limits to frequency and antenna size which place a lower limit on beamwidth for a given application.

The tracking error reduction methods considered here attempt to use the known relationship between the target and image geometry and signal characteristics to eliminate the multipath effect. The two methods examined are frequency agility and difference beam phase toggling.

B. FREQUENCY AGILITY

As mentioned above, the angle errors due to multipath at low elevations are cyclical. This is a result of the direct and surface-reflected signals reinforcing and canceling each other as the relative phase between two path varies. If the frequency is changed, the relative phases of the target and the image will change, and a new resultant is obtained as well as a new tracking error measurement. Thus the angle errors can be averaged by operating the radar over a wide frequency band or by sweeping the RF frequency and deducing the angle on the basis of the corresponding behavior of the error

38

signal. Since there is going to be a different error at each frequency, averaging the measurements at many frequencies might average out the errors.

The first attempt at reducing tracking error was in this direction, and the result shown in Figure 5.1 for uniform antenna coefficients. The final error estimate is obtained by finding the mean error for all frequencies. Comparing Figure 5.1 with Figure 4.3 shows that the error has been reduced significantly at most frequencies. However large errors still exist at large ranges.

A second attempt was made by taking measurements at a number of frequencies and then using the minimum and the maximum indicated elevations. The true elevation could be the midpoint or some other fraction of the indicated elevation angle. In the simulation
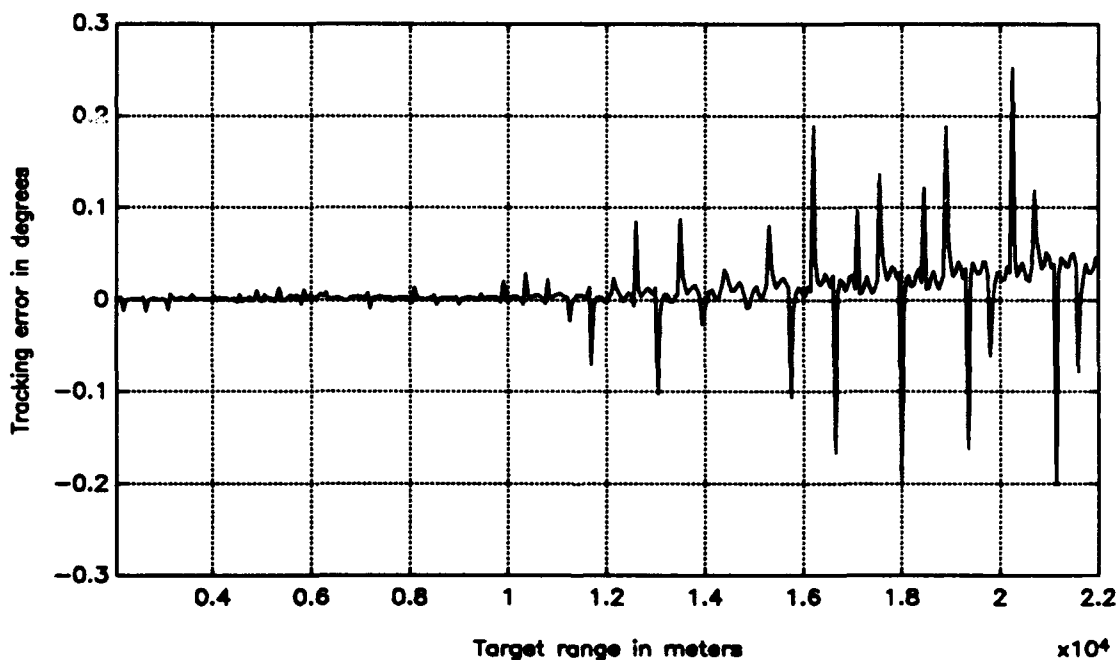
Figure 5.1 Reduced Tracking Error Using Uniform Coeffifcients. Frequency Agility with 20 Frequencies in 10 MHZ Increments and Averaging of Error Method is Used. Same Parameters as in Figure 4.3.

39

the minimum of the error is subtracted from the maximum value of the error over the whole range of frequencies. Half of this error is added to the minimum value. If i is the number of the agile frequencies then

$$Error = \frac{max(Error_i) - min(Error_i)}{2} + min(Error_i) \qquad (5\text{-}1)$$

A typical result is shown in Figure 5.2, and it is evident that the error is reduced even further. There is an overall improvement, but the greatest improvement occurs at low and high elevation angles.
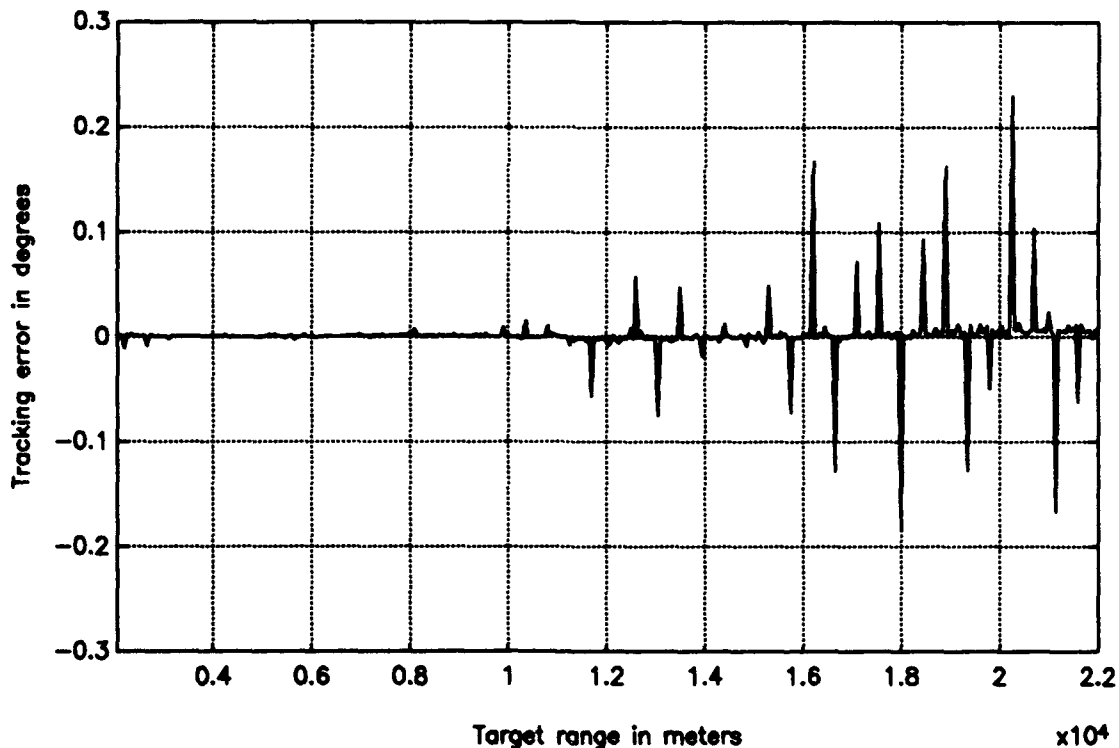
Figure 5.2 Reduced Tracking Error Using Uniform Coeffifcients, Frequency Agility with 20 Frequencies in 10 MHZ Increments and Maximum-Minimum Error Method is Used. Same Parameters as in Figure 4.3.

40

Both of the techniques have also been applied using Taylor and Bayliss antenna coefficients. The results are shown in Figures 5.3 and 5.4 for the averaging and maximum-minimum methods respectively.
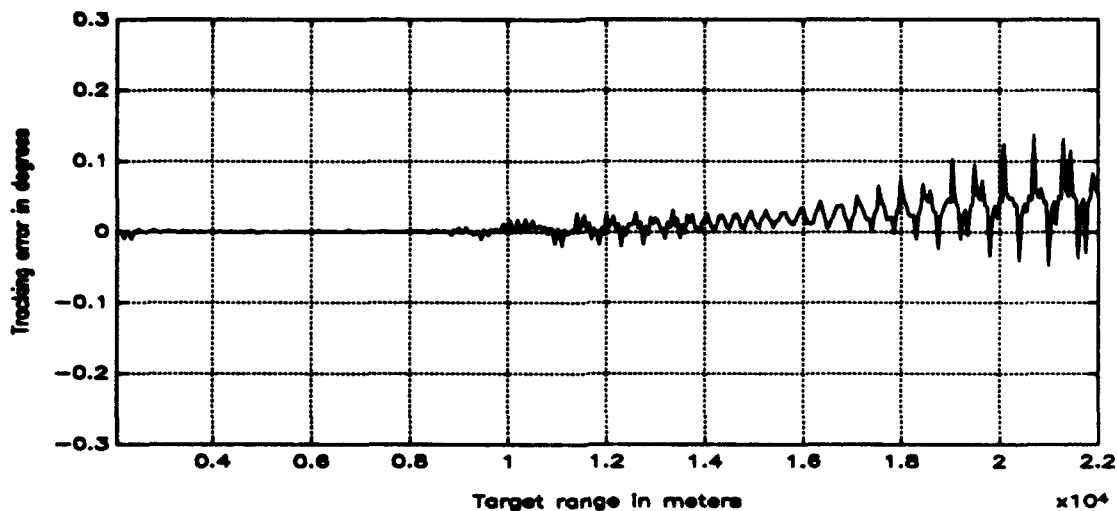
Figure 5.3 Reduced Tracking Error Using Taylor and Bayliss Coeffifcients, Frequency Agile with 20 Frequencies in 10 MHZ Increments and Averaging of Error Method is Used. Same Parameters as in Figure 4.3.
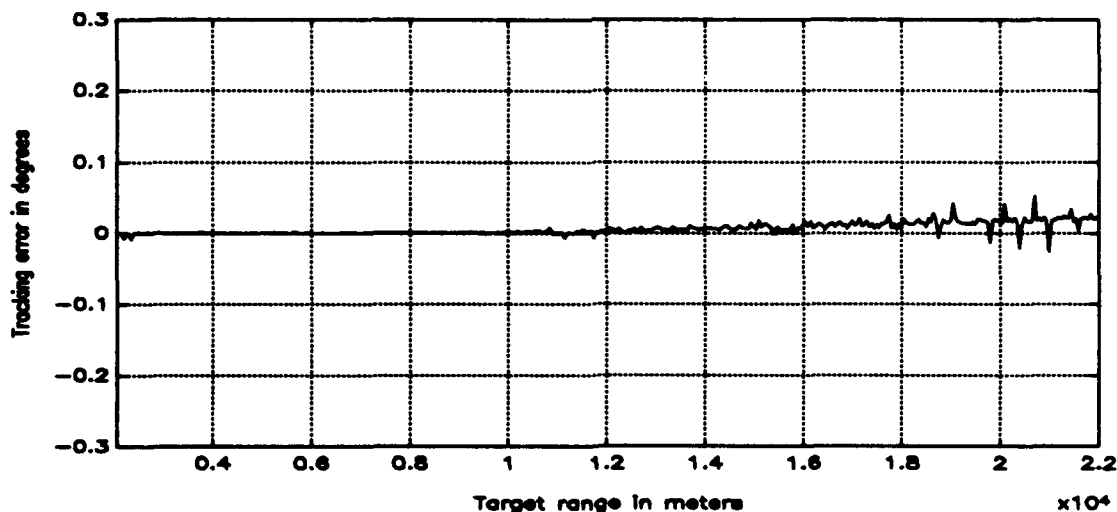
Figure 5.4 Reduced Tracking Error Using Taylor and Bayliss Coeffifcients, Frequency Agile with 20 Frequencies in 10 MHZ Increments and Maximum-Minimum Error Method is Used. Same Parameters as in Figure 4.3.

41

C.   DIFFERENCE BEAM PHASE TOGGLING METHOD

Difference beam phase toggling is a new method that compares the target returns from two successive pulses. However, the difference channel phase is flipped 180° for the second pulse. If the target parameters are the same from pulse to pulse and the antenna direction is close to the target, then the difference channel return will have only the main target return, while multipath components cancel.

The difference beam switching is illustrated in Figure 5.5. A multipath signal entering the difference beam lobe is shown with response Δ_i for pulse #1. When receiving the second pulse, the phase is flipped 180°. This can be done at RF by inserting a switch at the difference channel output, or digitally in the monopulse processor. If the multipath return does not change from pulse to pulse, then the multipath contribution will cancel. This assumes that the target RCS and location have not changed in the time interval between the two pulses. It also assumes that the direct target return is essentially nulled. If not, the target return will be cancelled similar to the multipath return. The radar will interpret this as the antenna being on target when in fact it is not.

The MATLAB simulation result for uniform antenna coefficients using this method is shown in Figure 5.6, and the result for Taylor and Bayliss coefficients is shown in Figure 5.7.

Comparing Figures 5.6 and 5.7 to the Figures 4.3 and 4.5 shows that the beam pointing error is reduced by approximately a half. Furthermore, this method is an easy signal processing upgrade for most monopulse radars.
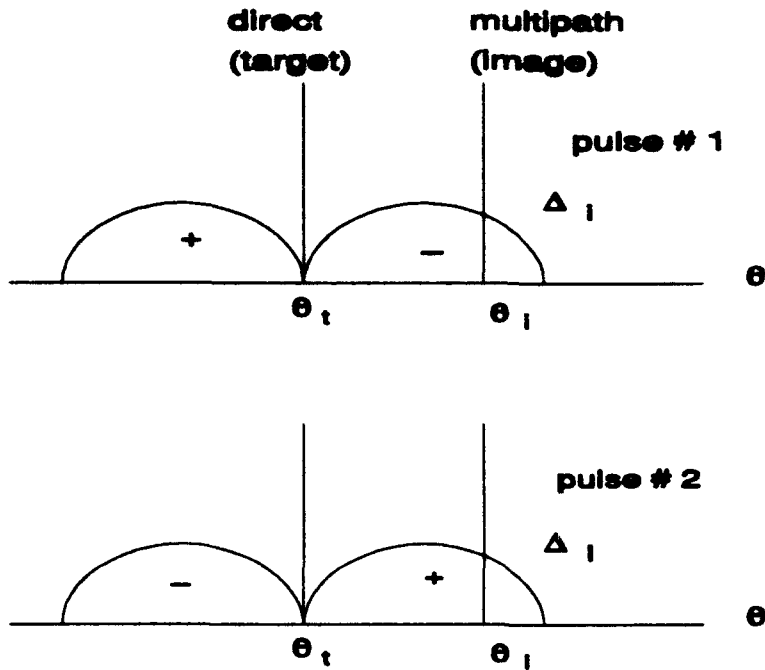
Figure 5.6 Difference Beam Response for Two Consecutive Pulses When the Phase is Toggled and Target is in the Null.
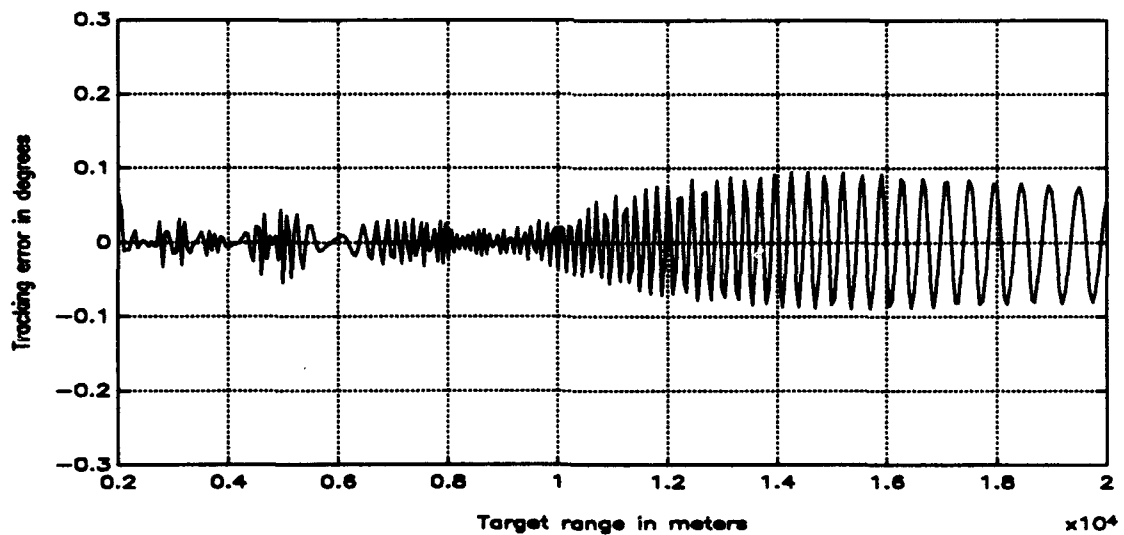
Figure 5.5 Reduced Tracking Error Using Difference Beam Phase Toggling for Uniform Antenna Coefficients. Same Parameters as in Figure 4.3.

43
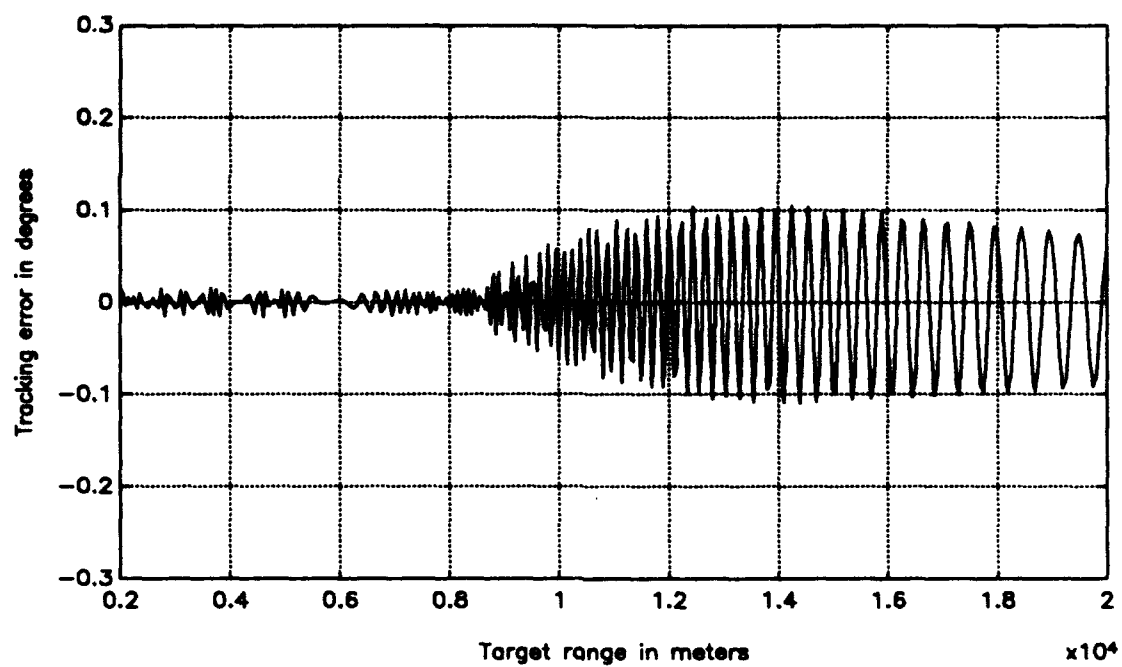
Figure 5.7 Reduced Tracking Error Using Difference Beam Phase Toggling Method for Taylor and Bayliss Antenna Coefficients. Same Parameters as in Figure 4.3.

VI. CONCLUSIONS AND RECOMMENDATIONS

At low elevation angles, both the direct and multipath reflected signals enter the main beam of the antenna and consequently monopulse receivers may indicate an erroneous target elevation estimate. The multipath scattering, antenna sum and difference responses, and the monopulse signal processor have been simulated using MATLAB. Both uniform and low sidelobe distributions have been considered.

The monopulse radar processor model was used to analyze the tracking error. The tracking error varied cyclically as the phase between the multipath and direct signals changed. As expected, the Taylor and Bayliss antenna coefficients resulted in less error because of lower sidelobes.

Two techniques have been used to reduce multipath error. The first method is frequency agility. Changing the transmitted frequency changed the relative phase of the two signals. When the frequency is changed in a systematic manner the tracking error as a function of frequency will be cyclic. Exploiting this property can reduce the error significantly at all but a few isolated ranges.

The second method used was the difference beam phase toggling which is a new method. It compares the target return from the two successive pulses. The simulation data indicates that tracking over a smooth surface can be improved by at least a factor of two. Frequency agility requires considerable modification of conventional narrowband monopulse tracking radars. On the other hand, difference beam phase toggling can be

implemented by a simple modification in the processing of angle-error signals. Thus it is relatively easy to implement in existing systems.

The phase toggling method works well when the antenna is initially trained on the target. Further research should investigate its performance when the target is significantly off boresight at the start of track.

Another approach to reducing errors is to fuse the data output from different sensors such as TV, IR, or lasers with that of the radar. Although they may improve the tracking accuracy, these devices have limited range and cannot operate in all weather conditions.

APPENDIX A   MATLAB UNIFORM DISTRIBUTION PROGRAM

```
********************************************************************
*This program calculates the array factor of the sum and difference pattern of a
*monopulse antenna. Using the array factor the sum and the difference patterns are
*plotted.
*FILENAME : Sdunid.m
********************************************************************
clear;
clg;
nel=input('Enter number of the antenna elements = ');
slldb=input('Enter side lobe level in dB = ');
ts=input('Enter scan angle = ');
nbar=input('Enter nbar = ');
d=input('Enter element distance in wavelength = ');
ts=sin(pi*ts/180);
********************************************************************
*This part is for difference pattern.
********************************************************************
for i = 1:nel/2
      rho =( 2*i-1) / nel;
      amp(nel/2+1-i) =1;
      amp(nel/2 + i) =1;
end
amp=amp/max(amp);
it=0;
for t=-90:0.5:90
      it=it+1;
      ang(it)=t;
      af(it)=0;
            for n=1:nel
                ph=0;
                     if n>nel/2
                            ph=pi;
                     end
                af(it)=af(it)+amp(n)*exp(j*(n-1)*2*pi*d*(sin(pi*t/180)-ts)+j*ph);
            end;
end
afdb=max(10*log(abs(af)),-60);
plot(ang,afdb);
```

```
xlabel('Angle in degrees');
ylabel('AF magnitude (dB)');
grid;
pause;
********************************************************************
*This part is for sum pattern.
********************************************************************
amp1=ones(1,nel);
amp1=amp1/max(amp1);
it1=0;
for t=-90:0.5:90
      it1=it1+1;
      ang1(it1)=t;
      af1(it1)=0;
            for n=1:nel
                  af1(it1)=af1(it1)+amp1(n)*exp(j*(n-1)*2*pi*d*(sin(pi*t/180)-ts));
            end
end
af1db=max(10*log(abs(af1 )),-60);
plot(ang1,af1db);
xlabel('Angle in degrees');
ylabel('AF magnitude (dB)');
grid;
pause;
```

APPENDIX B - MATLAB TAYLOR DISTRIBUTION FUNCTION

```
*******************************************************************
  function a=taylor(slr,n_bar,N)
*******************************************************************
```

*This function calculates amplitude weight coefficients for an n element array based
*on Taylor amplitude distribution. The input arguments are the desired main lobe -
*sidelobe ratio (dB), the sidelobe parameter n_bar, and the number of array
*elements. The output variable is the amplitude weights an. The procedure is outlined
*in thr text "The Handbook of Antenna Design (vol.2)" edited by A. W. Rudge, K.
*Milne, A.D Olver, and P. Knight.

```
 p=n_bar-1;
dbamp=20/log(10);
sll=exp(abs(slr)/dbamp);
A=(1/pi)*log(sll+sqrt(sll.^2-1));
sigma=n_bar/(sqrt(A.^2+(n_bar-1/2).^2));
f=ones(p,1);
for m=1:p
      z(m)=sigma*sqrt(A.^2+(m-1/2).^2);
      K(m)=(fact(p)).^2./(fact(p+m).*fact(p-m));
end
for n=1:p
      P(n)=prod(1-(n.^2 ./z.^2));
end
f=K.*P;
J=zeros(N/2,p);
for i=1:N/2
      for k=1:p
             J(i,k)=f(:,k).*cos(k.*pi.*2*(i-1)/N);
      end
end
g=1+2*sum(J.');
a=[fliplr(g) g].';
a=a/max(a);
```

```
******************************************************************
*This part of the program is just for using the function called Taylor and ploting the
*Taylor sum pattern of a monopulse antenna.
*FILENAME : Sumtay.m
******************************************************************
clear;
clg;
nel=input('Enter number of the antenna elements = ');
slldb=input('Enter side lobe level in dB = ');
ts=input('Enter scan angle = ');
nbar=input('Enter nbar = ');
d=input('Enter element distance in wavelength = ');
ts=sin(pi*ts/180);

amp1=0;
amp1= abs(taylor(slldb,nbar,nel));

 it1=0;
for t=-90:0.1:90
      it1=it1+1;
      angle1(it1)=t;
      af1(it1)=0;
            for n=1:nel
                  af1(it1)=af1(it1)+amp1(n)*exp(j*(n-1)*2*pi*d*(sin(pi*t/180)-ts));
            end
end
plot(angle1,10*log(abs(af1)));
xlabel('Angle in degrees');
ylabel('AF magnitude (dB)');
grid;
```

50

APPENDIX C - MATLAB BAYLISS DISTRIBUTION FUNCTION

```
************************************************************************
function amp=bayliss(rho,sll,nbar)
************************************************************************
```

*This function calculates amplitude weight coefficients for an n element array based
*on Bayliss amplitude distribution. The input arguments are desired main lobe - side
*lobe ratio (dB), the sidelobe parameter n_bar, and the number of array elements.The
*output variable is the amplitude weights an.

```
nbar1 = nbar-1;
for i=1:11
        mu(i) = i-1 +.5;
end
sll25 = sll-25;
z(1) = 1.87 + sll25 * (.038);
z(2) = 2.5 + sll25 * (.016);
z(3) = 3.35 + sll25 * (.019);
z(4) = 4.25 + sll25 * (.016);
a = 1.45 + sll25 * (.042);
for ns = 5:nbar
    ans = ns;
    z(ns) = (a*a+ans^2)^.5;
end
sigma = mu(nbar+1) / z(nbar);
for mms = 1:nbar
    bb = 1:
        1 :. ns = 1:nbar1
                bb =bb*(1-(mu(mms)/(sigma*z(ns)))^2);
        end
    bbb = 1;
        for lls = 1:nbar
            dum = lls - mms;
                if dum~=0
                        bbb = bbb * (1-(mu(mms) / mu(lls))^2);
                end;
        end
    bes = (-1) ^ mms;
    b(mms) = mu(mms)^2 / bes*bb / bbb;
end
```

```
gg = 0;
for lls = 1:nbar
      pmu = mu(lls) * pi * rho;
      bes = sin(pmu);
      gg = gg + b(lls) * bes;
end
amp = gg;


***********************************************************************
*This part of the program is just for using the function called Bayliss and ploting the
*Bayliss difference pattern of a monopulse antenna.
*FILENAME : Difbay.m
***********************************************************************
clear;
clg;
nel=input('Enter number of the antenna elements = ');
slldb=input('Enter side lobe level in dB = ');
ts=input('Enter scan angle = ');
nbar=input('Enter nbar = ');
d=input('Enter element distance in wavelength = ');
ts=sin(pi*ts/180);
for i = 1:nel/2
      rho =( 2*i-1) / nel;
      amp(nel/2+1-i) = abs(bayliss(rho,slldb,nbar));
      amp(nel/2 + i) = abs(bayliss(rho,slldb,nbar));
end
it=0;
for t=-90:0.1:90
      it=it+1;
      angle(it)=t;
      af(it)=0;
            for n=1:nel
               ph=0;
                     if n>nel/2
                           ph=pi;
                     end
               af(it)=af(it)+amp(n)*exp(j*(n-1)*2*pi*d*(sin(pi*t/180)-ts)+j*ph);
            end
end
plot(angle,10*log(abs(af)));
xlabel('Angle in degrees');
ylabel('AF magnitude (dB)');
grid;pause;
```

APPENDIX D-MONOPULSE TRACKING ERROR PROGRAM FOR TAYLOR

AND BAYLISS COEFFICIENTS

```
*******************************************************************
*This program calculates the real value of difference to sum ratio of a monopulse
*antenna pattern using Taylor and Bayliss coefficients. The calulation is made for a
*flying out in range and constant altitude target.
*FILENAME : Tez1d.m
*******************************************************************
clear;
clg;
nel=input('Enter number of the antenna elements = ');
slldb=input('Enter side lobe level in dB = ');
ts=input('Enter scan angle = ');
 nbar=input('Enter nbar = ');
 d=input('Enter element distance in wavelength = ');
 ts=sin(pi*ts/180);
*******************************************************************


*Generating Bayliss coefficients for difference pattern.
*******************************************************************
for i = 1:nel/2
      rho =( 2*i-1) / nel;
      amp(nel/2+1-i) = abs(bayliss(rho,slldb,nbar));
      amp(nel/2 + i) = abs(bayliss(rho,slldb,nbar));
end
amp=amp/max(amp);
*******************************************************************


*Generating Taylor coefficients for sum pattern.
*******************************************************************
amp1=0;
amp1= abs(taylor(slldb,nbar,nel));
amp1=amp1/max(amp1);
f=9e9;
la=3e8/f;
h1=input('enter radar height = ');
h2=input('enter target height = ');
a=input('enter magnitude of relection coefficient = ');
```

```
ang=input('enter phase angle of reflection coefficient = ');
l=2000:50:20000;
r1=((h2-h1)^2+l.^2).^(1/2);
teta=atan((h2-h1)*ones(1,length(l))./l);
alfa=-atan(sqrt(((h1+h2)^2)*ones(1,length(l))./(r1.^2-(h2-h1)^2)));
r2=(h1+h2)*ones(1,length(l))./sin(alfa);
fhi=2*pi*(r2-r1)/la;


*****************************************************************
*Generating difference pattern.
*****************************************************************
difft=0;
diffi=0;
e=0;
sumi=0;
sumt=0;
totdif=0;
totsum=0;
for i=1:length(alfa)
        for n=1:nel
                ph=0;
                    if n>nel/2
                            ph=pi;
                    end
                    if i==1
                    difft=difft+amp(n)*exp(j*(n-1)*2*pi*d*(sin(teta(i))-sin(teta(i)))+j*ph);
                    diffi=diffi+amp(n)*exp(j*(n-1)*2*pi*d*(sin(alfa(i))-sin(teta(i)))+j*ph);
                    else
        difft=difft+amp(n)*exp(j*(n-1)*2*pi*d*(sin(teta(i))-sin(teta(i-1)-erad(i-1)))+j*ph);
        diffi=diffi+amp(n)*exp(j*(n-1)*2*pi*d*(sin(alfa(i))-sin(teta(i-1)-erad(i-1)))+j*ph);
                    end
 end


*****************************************************************
*Generating sum pattern.
*****************************************************************
for n=1:nel
        if i==1
                sumt=sumt+amp1(n)*exp(j*(n-1)*2*pi*d*(sin(teta(i))-sin(teta(i))));
                sumi=sumi+amp1(n)*exp(j*(n-1)*2*pi*d*(sin(alfa(i))-sin(teta(i))));
        else
```

```
           sumt=sumt+ampl(n)*exp(j*(n-1)*2*pi*d*(sin(teta(i))-sin(teta(i-1)-erad(i-1))));

sumi=sumi+ampl(n)*exp(j*(n-1)*2*pi*d*(sin(alfa(i))-sin(teta(i-1)-erad(i-1))));  erd
end
*****************************************************************************
*Calculation of error using total sum and total difference
*****************************************************************************
totsum=sumt+ a*exp(j*(ang+fhi(i)))*sumi;
totdif=difft+a*exp(j*(ang+fhi(i)))*diffi;
e(i)=real(totdif/totsum);
erad(i)=e(i)*pi/180;
end
plot(l,e);
xlabel('range');
ylabel('elevation error in degrees')
grid;
```

APPENDIX E-MONOPULSE TRACKING ERROR PROGRAM FOR UNIFORM

AMPLITUDE ANTENNA COEFFICIENTS

```
**********************************************************************
*This program calculates the real value of difference to sum ratio of a monopulse
*antenna pattern using uniform coefficients. The calulation is made for a flying out in
*range and constant altitude target.
*FILENAME : Tezuni.m
**********************************************************************
clear;
clg;
nel=input('Enter number of the antenna elements = ');
slldb=input('Enter side lobe level in dB = ');
ts=input('Enter scan angle = ');
 nbar=input('Enter nbar = ');
 d=input('Enter element distance in wavelength = ');
 ts=sin(pi*ts/180);
**********************************************************************


*Generating uniform coefficients for difference pattern.
**********************************************************************
for i = 1:nel/2
      rho =( 2*i-1) / nel;
      amp(nel/2+1-i) =1;
      amp(nel/2 + i) =1;
end
amp=amp/max(amp);
**********************************************************************


*Generating uniform coefficients for sum pattern.
**********************************************************************
amp1=ones(1,nel);
f=9e9;
la=3e8/f;
h1=input('enter radar height = ');
h2=input('enter target height = ');
a=input('enter magnitude of relection coefficient = ');
ang=input('e  _ phase angle of reflection coefficient = ');
 l=2000:50:20000;
```

```
r1=((h2-h1)^2+l.^2).^(1/2);
teta=atan((h2-h1)*ones(1,length(l))./l);
alfa=-atan(sqrt(((h1+h2)^2)*ones(1,length(l))./(r1.^2-(h2-h1)^2)));
r2=(h1+h2)*ones(1,length(l))./sin(alfa);
fhi=2*pi*(r2-r1)/la;


***********************************************************************
*Generating difference pattern.
***********************************************************************
difft=0;
diffi=0;
e=0;
sumi=0;
sumt=0;
totdif=0;
totsum=0;
for i=1:length(alfa)
      for n=1:nel
            ph=0;
                if n>nel/2
                      ph=pi;
                end
                if i==1
                difft=difft+amp(n)*exp(j*(n-1)*2*pi*d*(sin(teta(i))-sin(teta(i)))+j*ph);
                diffi=diffi+amp(n)*exp(j*(n-1)*2*pi*d*(sin(alfa(i))-sin(teta(i)))+j*ph);
                else
        difft=difft+amp(n)*exp(j*(n-1)*2*pi*d*(sin(teta(i))-sin(teta(i-1)-erad(i-1)))+j*ph);
        diffi=diffi+amp(n)*exp(j*(n-1)*2*pi*d*(sin(alfa(i))-sin(teta(i-1)-erad(i-1)))+j*ph);
                end
 end


***********************************************************************
*Generating sum pattern.
***********************************************************************
for n=1:nel
      if i==1
            sumt=sumt+amp1(n)*exp(j*(n-1)*2*pi*d*(sin(teta(i))-sin(teta(i))));
            sumi=sumi+amp1(n)*exp(j*(n-1)*2*pi*d*(sin(alfa(i))-sin(teta(i))));
      else

sumt=sumt+amp1(n)*exp(j*(n-1)*2*pi*d*(sin(teta(i))-sin(teta(i-1)-erad(i-1))));

sumi=sumi+amp1(n)*exp(j*(n-1)*2*pi*d*(sin(alfa(i))-sin(teta(i-1)-erad(i-1))));  end
```

```
end
******************************************************************
*Calculation of error using total sum and total difference
******************************************************************
totsum=sumt+ a*exp(j*(ang+fhi(i)))*sumi;
totdif=difft+a*exp(j*(ang+fhi(i)))*diffi;
e(i)=real(totdif/totsum);
erad(i)=e(i)*pi/180;
end
plot(l,e);
xlabel('Target range');
ylabel('Tracking error in degrees')
grid;
```

LIST OF REFERENCES

1. Levanon, Nadav, *Radar Principles*, pp. 68-78, pp. 285-301, John Wiley & Sons Inc., 1988.

2. Barton, David K., *Radar Resolution and Multipath Effects*, 2nd. ed., pp. 27-35, Artech House, Inc., 1984.

3. Hovanessian, S. A., *Radar System Design and Analysis*, pp. 173-187, Artech House, Inc., 1984.

4. Rhodes, Donald R., *Introduction to Monopulse*, Artech House, Inc., 1980.

5. Skolnik, Merrill I., *Introduction to Radar Systems*, pp. 152-186, McGraw-Hill Publishing Company, 1980.

6. Sherman, Samuel M., *Monopulse Principles and Techniques*, pp. 129-148, Artech House, Inc., 1984.

7. Balanis, Constantine A., *Antenna Theory Analysis and Design*, pp.679-682, John Wiley & Sons, 1982.

8. Elliott, Robert S., *Antenna Theory and Design*, pp. 181-193, Prentice-Hall, Inc., 1981.

INITIAL DISTRIBUTION LIST

No. Copies

1. Defense Technical Information Center   2
    Cameron Station
    Alexandria VA 22304-6145

2. Library, Code 52   2
    Naval Postgraduate School
    Monterey CA 93943-5101

3. Chairman, Code EW   1
    Electronic Warfare Academic Group
    Naval Postgraduate School
    Monterey, CA 93943-5121

4. Professor David C. Jenn, Code EC/JN   2
    Department of Electrical and Computer Engineering
    Naval Postgraduate School
    Monterey, CA 93943-5121

5. Professor Gurnam Gill, Code EC/GL   1
    Department of Electrical and Computer Engineering
    Naval Postgraduate School
    Monterey, CA 93943-5121

6. Deniz Kuvvetleri Komutanligi   1
    Personel Daire Baskanligi
    Bakanliklar, Ankara, Turkey

7. Deniz Harp Okulu Komutanligi   1
    Tuzla, Istanbul, Turkey

8. Golcuk Tersanesi Komutanligi   1
    Golcuk, Kocaeli, Turkey

9. Taskizak Tersanesi Komutanligi   1
    Haskoy, Istanbul, Turkey

10.   Ali Ozkara   1
        Cinili Hamam Sok. No:50/12
        Uskudar, Istanbul, Turkey 81140